Geological Magazine

www.cambridge.org/geo

Sb–Au-bearing chalcedonies in hot geothermal systems: insights from the jasperoids of Poggio Peloso (southern Tuscany, Italy)

Elisabetta Gliozzo[1], Andrea Brogi[2,3], Giovanni Ruggieri[4] and Antonio Langone[5,6]

[1]Department of Humanities Research and Innovation, University of Bari, Bari 70121, Italy; [2]Department of Earth and Geoenvironmental Sciences, University of Bari, Bari 70121, Italy; [3]CNR – Institute of Geosciences and Earth Resources, Pisa 56121, Italy; [4]CNR – Institute of Geosciences and Earth Resources, Florence 50100, Italy; [5]CNR – Institute of Geosciences and Earth Resources, Pavia 27100, Italy and [6]Department of Earth and Environmental Sciences, University of Pavia, Pavia 27100, Italy

Original Article

Cite this article: Gliozzo E, Brogi A, Ruggieri G, and Langone A (2023) Sb–Au-bearing chalcedonies in hot geothermal systems: insights from the jasperoids of Poggio Peloso (southern Tuscany, Italy). *Geological Magazine* **160**: 712–731. https://doi.org/10.1017/S0016756822001200

Received: 4 February 2022
Revised: 13 September 2022
Accepted: 5 November 2022
First published online: 16 January 2023

Keywords:
Sb–Au deposits; jasperoid; Pietratonda–Poggio Peloso; Sb-mineralization; geothermal fluids

Author for correspondence:
Elisabetta Gliozzo,
Email: Elisabetta.gliozzo@uniba.it

Abstract

Detailed characterization was performed on the chalcedonies from the jasperoids of the Pietratonda–Poggio Peloso Sb–Au deposit (southern Tuscany, Italy). The main purpose was to retrieve information on the geothermal fluids that formed the chalcedonies and the source of antimony concentrations. Investigations were performed using optical microscopy, laser ablation inductively coupled plasma mass spectroscopy and X-ray diffraction on both the chalcedonies and the lithotypes cropping out in the area. The results obtained allow the chalcedonies of Pietratonda–Poggio Peloso to be described as a *unicum*, based on the very high contents of Sb that do not find a comparison in the literature. The textures showed multiple generations of silica that agree well with an environment characterized by multiple injections of mineralizing solutions, bearing variable physicochemical characteristics. The transport likely took place in an alkaline environment, while the acidification of the water may have favoured the precipitation at varying temperatures but not higher than 225 °C. The rocks from which the constituents may have been leached are the hosting carbonates and the surrounding metamorphic rocks. Among the examined rocks, the metamorphic rocks showed the most numerous and significant correspondences with the chalcedonies and were the only ones in which discrete amounts of gold contents were found.

1. Introduction

Jasperoids consist of silica formed by metasomatic carbonate replacement from fluid–rock interaction (Lovering, 1962) in active geothermal systems. In continental settings, many geothermal systems are hosted in carbonate rock volumes that play the role of extensive reservoirs (Barbier, 2002; Faulds *et al.* 2011; Garland *et al.* 2012; Brogi *et al.* 2016). Carbonate rocks, in fact, are prone to forming permeable volumes if interconnected fractures develop during their deformation (e.g. Agosta *et al.* 2010). It occurs when carbonate rocks are involved in tectonic events at relatively low temperatures (i.e. in the upper crustal level), as in the case of extensional processes triggering detachment zones (Carmignani *et al.* 2001; Brogi & Cerboneschi, 2007; Matera *et al.* 2021). In these geological contexts, the carbonate units can offer suitable secondary permeability to host significant volumes of geothermal fluids (Romagnoli *et al.* 2010; Brogi *et al.* 2020) and, depending on their chemical features, react with them, depositing neoformational minerals (i.e. banded calcite veins: Hancock *et al.* 1999; Capezzuoli *et al.* 2018; Brogi *et al.* 2021) and jasperoids. Jasperoid formation is often associated with ore development mainly consisting of antimony and gold deposits (Dessau, 1952, 1977; Klemm & Neumann, 1984; Bagby & Berger, 1985; Tanelli *et al.* 1991; Cline & Hofstra, 2000; Cline *et al.* 2005; Sillitoe & Brogi, 2021). This is the case for southern Tuscany where jasperoids consist of extensive stratabound volumes (Lattanzi, 1999; Brogi *et al.* 2011; Brogi & Fulignati, 2012; Morteani *et al.* 2017) confined between low-permeability units, developed in correspondence with cataclastic horizons formed during the Neogene–Quaternary extensional evolution of the inner Northern Apennines (Carmignani *et al.* 1994; Brogi *et al.* 2005). Nevertheless, the metasomatic process triggering the formation of jasperoids and Sb–Au deposition is the result of repeated pulses of fluid injection within the hosting rocks, a consequence of the tectonically controlled dynamic evolution of the geothermal system.

The study of chalcedony and agate generally addresses multiple objectives such as the identification of the sources of the elements, the characterization of the fluids and the reconstruction of the mobilization, transport, precipitation and depositional conditions. The study of chalcedony represents a flourishing research topic, prompting international interest. Several scholars have contributed to the knowledge of these materials, providing essential information on

their composition, microstructure and banding (see, e.g. Heaney, 1993; Graetsch, 1994; Heaney *et al.* 1994; Heaney & Davis, 1995; Merino *et al.* 1995; Wang & Merino, 1995; Götze *et al.* 1998; French *et al.* 2003). Various studies have also been focused on the investigation of their genesis in volcanic (see, e.g. Götze *et al.* 2001, 2016; Gilg *et al.* 2003; Moxon & Reed, 2006; Dumańska Słowik *et al.* 2008; Richter *et al.* 2015) and sedimentary environments (see, e.g. Moxon & Reed 2006; Götze *et al.* 2009). Furthermore, the widespread distribution of chalcedony in correspondence with meso- to epithermal ore deposits has also favoured research on polymetallic (Sb, Zn, Pb, Au, Ag) vein-type ore deposits (see, e.g. Dill *et al.* 2008; Moreira & Fernandez 2015; Radosavljević *et al.* 2016).

The studies performed on chalcedonies indicate that the deposition temperatures range from 20 to 230 °C (Harris, 1989; Fallick *et al.* 1985; Saunders, 1990; Heaney, 1993; Götze *et al.* 2020) and that, in sedimentary and low-temperature hydrothermal environments, near-surface conditions are the most favourable for their formation (see, e.g. White & Corwin, 1961; Cady *et al.* 1998). In the area under examination, a few studies performed on quartz fluid inclusions estimated homogenization temperatures ranging between 125 ± 3 and 232 °C (unpub. studies performed by Roedder on quartz from Poggio Fuoco, mentioned by Dessau *et al.* 1972), between 140 and 232 °C (quartz from Pereta) or between 155 and 255 °C (quartz from Poggio Peloso in Brogi & Fulignati, 2012). These temperatures are close to those stated for stibnite precipitation, which has been constrained to between 132 and 245 °C by Lattanzi (1999) and confirmed at 250 °C by Morteani *et al.* (2017).

Following the work previously carried out in this area, this paper presents results of the study of the chalcedonies from the Pietratonda–Poggio Peloso Sb–Au epithermal mineralization (southern Tuscany, Italy; Fig. 1), which consists of an exhumed hot geothermal system developed during Quaternary time (Brogi & Fulignati, 2012). The main purposes of the study are: (1) to investigate the origin of antimony, gold and other elements present in the examined chalcedonies, by comparing the geochemical features and rare earth element (REE) patterns of the chalcedonies and selected lithotypes which may have reacted with the fluids that deposited the chalcedonies and, (2) to obtain information on the depositional environment of the chalcedonies. To these aims, optical and X-ray diffraction analyses were carried out and major, minor and trace elements were determined on six samples of chalcedonies and 11 samples from selected lithotypes, by laser ablation inductively coupled plasma mass spectroscopy (LA-ICP-MS) and X-ray fluorescence (XRF).

2. Geological outline

2.a. Southern Tuscany in the inner Northern Apennines

Southern Tuscany is part of the inner zone of the Northern Apennines orogen (Fig. 1), a Tertiary fold-thrust belt formed during collision between the Adria microplate (part of the African plate) and the Corsica–Sardinia massif (related to the European plate). Late Cretaceous through early Oligocene convergence of the African and European plates by subduction of the intervening western Tethys Ocean led to late Oligocene – early Miocene collision and eastward transport and emplacement of a thrust stack (see, e.g. Molli, 2008). The Northern Apennines stack is formed, from the top down by (1) Jurassic–Cretaceous ophiolite and pelagic sedimentary cover of the Tethyan oceanic realm (Ligurian units, LU) and (2) Cretaceous–Oligocene turbidites representing the continent–ocean transition (Sub-Ligurian units, SLU), both of which were thrust in late Oligocene – early Miocene times over (3) the Upper Triassic to lower Miocene evaporite, carbonate, terrigenous and marine siliciclastic succession of the Adria passive margin (Tuscan Nappe, TN2). The evaporite level of the Tuscan Nappe is made up of partly de-dolomitized, anhydrite-dolostone breccia (known as the Calcare Cavernoso and Burano formations, TN1); its highly permeable and vacuolar texture is due to the interplay among different processes, such as cataclasis, anhydrite dissolution and karstification (see, e.g. Gandin *et al.* 2000). During early Miocene time, the Tuscan Nappe was thrust over (4) the polydeformed blueschist- to greenschist-facies (Giorgetti *et al.* 1998; Brogi & Giorgetti, 2012) tectonic wedge complex (known as the Tuscan metamorphic complex; Pandeli *et al.* 1991) made up of phyllite and metaquartzite of Early to Middle Triassic age (Verrucano Group, MRU3), which overlies (5) phyllite and metacarbonate derived from Carboniferous–Permian protoliths (MRU2). MRU2 overlies (6) Precambrian to early Palaeozoic micaschist (MRU1) and (7) gneissic basement with Precambrian to early Palaeozoic protoliths. Locally, the thrusting caused interleaving of the Calcare Cavernoso and underlying metamorphic units, especially in the upper part of the tectonic wedge complex.

Beginning in early Miocene time, the previously stacked units were affected by extension (Carmignani *et al.* 2001). Extension produced: (a) lateral segmentation of the previously stacked units and formation of bowl-shaped basins (Brogi & Liotta, 2008; Brogi, 2011); and (b) development of NW-striking Pliocene–Quaternary normal faults, cross-cutting all the previous structures and inducing development of NW-trending tectonic depressions, filled by continental and marine sediments (Martini & Sagri, 1993; Brogi *et al.* 2013; Martini *et al.* 2021). The primary evidence of extension is the opening of the Tyrrhenian Basin (Bartole, 1995) and the present crustal and lithospheric thicknesses of ~17 and 40 km, respectively (Calcagnile & Panza, 1981; Locardi & Nicolich, 1982; Di Stefano *et al.* 2011; Möller *et al.* 2013).

At least since Langhian time, extension was accompanied by eastward migrating magmatism (Serri *et al.* 1993). It affected the area corresponding to the Tuscan archipelago and the inland inner Northern Apennines (Serri *et al.* 2001; Dini *et al.* 2005, 2008). Magmas were emplaced at shallow crustal levels (6–8 km depth, mainly: Serri *et al.* 2001) mostly along NE-striking brittle shear zones playing the role of transfer zones (Dini *et al.* 2008). Hot geothermal systems (T >200 °C) developed near the intrusive bodies and are now exposed in the whole Tuscan archipelago and southern Tuscany (e.g. Liotta *et al.* 2010; Vezzoni *et al.* 2016; Zucchi *et al.* 2017; Zucchi, 2020). Active systems are presently exploited at depth for geothermal energy production (cf. Liotta *et al.* 2021) in the Larderello and Monte Amiata areas (Batini *et al.* 2003 and references therein).

2.b. The Pietratonda–Poggio Peloso area

The Pietratonda–Poggio Peloso area (Fig. 1) is mainly characterized by exposures of jasperoid that formed by the silica replacement of the basal Upper Triassic evaporitic horizon of the Tuscan Nappe (Bernoulli, 2001). This level tectonically overlies the Triassic continental metasiliciclastic succession of the Verrucano Group mainly consisting of quartzite and phyllite with metacarbonate and phyllite at the top (Meccheri *et al.* 1987; Moretti, 1991; Aldinucci *et al.* 2005), which recorded a polyphase tectonometamorphic evolution (Aldinucci *et al.* 2005; Brogi, 2006).

https://doi.org/10.1017/S0016756822001200 Published online by Cambridge University Press

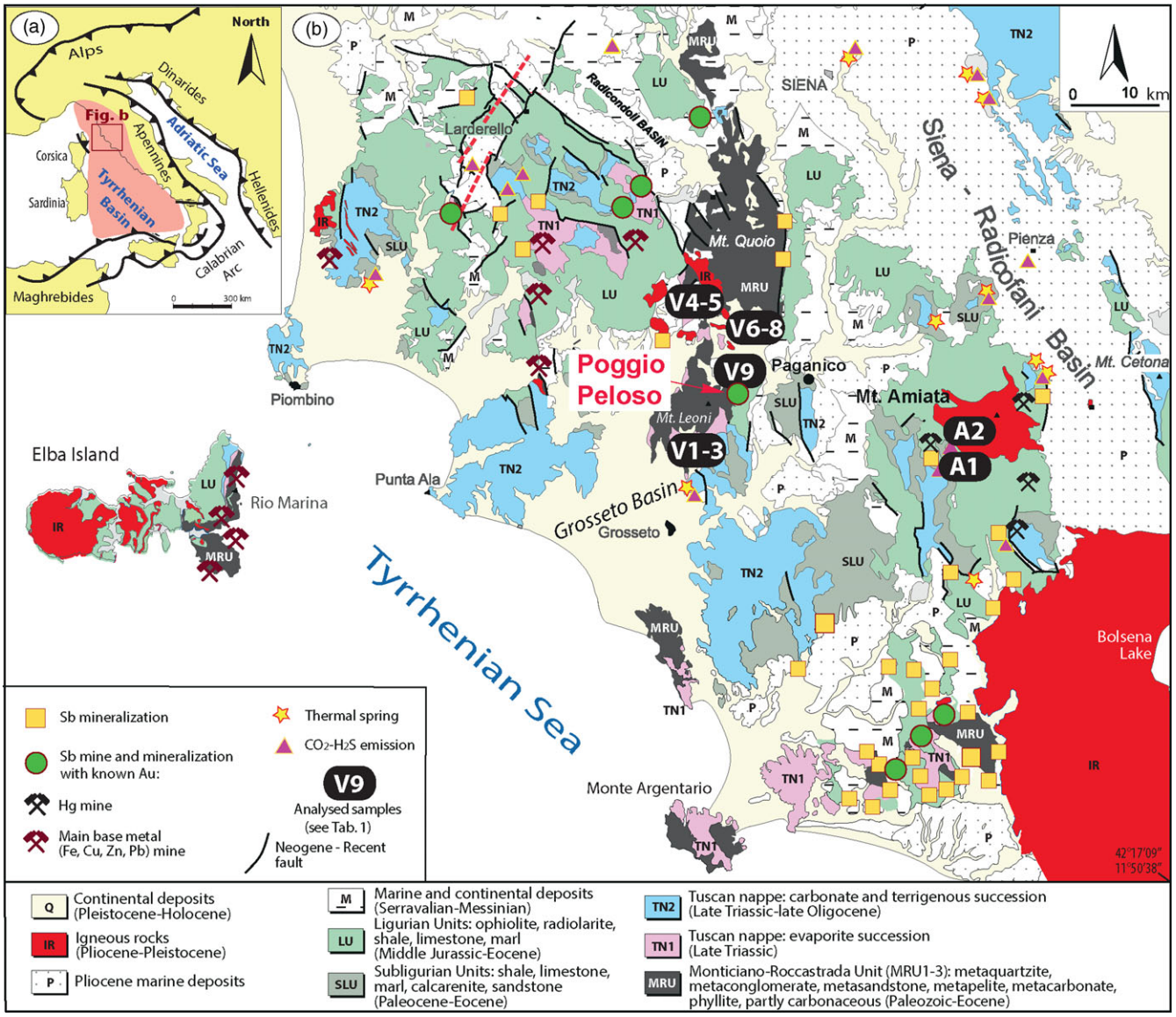

Fig. 1. (Colour online) The geographic distribution of Sb-mineralization in southern Tuscany and northern Lazio. The sampling sites are indicated by the name of the sample except for the chalcedonies (all taken from Poggio Peloso).

At the top of the jasperoid level, discontinuous bodies made up of upper Oligocene – lower Miocene quartz–feldspar sandstone (Macigno Fm) occur. The contact juxtaposing the Macigno Fm on the jasperoid is tectonic and corresponds to a low-angle normal fault (Brogi, 2008). On top, Ligurian units and Miocene sediments formed the cap of the palaeo-geothermal system that was controlled by WSW–ENE strike-/oblique-slip and NNE–SSW normal faults, forming linkage zones between the main strike-slip fault segments (Brogi & Fulignati, 2012). The geothermal fluids consisted of meteoric water circulated to depth and heated owing to the geothermal anomaly. According to Brogi & Fulignati (2012), these fluids reached temperatures of ~200–225 °C and a maximum salinity of ~3 wt % NaCl equiv.

2.c. Sb-mineralization and disseminated gold

Southern Tuscany has represented one of the most important mining districts of the Mediterranean basin from the Etruscan period to the twentieth century, with a limited time break during the Roman Empire. Deposits of pyrite, iron, lead, zinc and minor silver and gold are widespread and typically related to the activity of geothermal fluids associated with the Neogene–Quaternary magmatism (Tanelli, 1983; Tanelli *et al.* 1991; Serri *et al.* 1993; Lattanzi, 1999; Peccerillo *et al.* 2001; Dini, 2003; Peccerillo, 2003; Dini *et al.* 2005; Boschi *et al.* 2009). The most significant Sb-ore sources are typically located along the NE–SW strip connecting Mount Amiata with Capalbio; however, further deposits are located north of the area of concentration (Fig. 1). The distribution of Sb-deposits shows common features throughout the area: (1) the distribution includes the peripheral zones of present and fossil geothermal areas, coinciding with a Sb mineralized belt; (2) they are associated with fluid flow channelled by extensional faults (Dessau *et al.* 1972; Tanelli, 1983; Tanelli & Scarsella, 1990; Tanelli *et al.* 1991; Brogi *et al.* 2011; Brogi & Fulignati, 2012); (3) they are typically found at the contact between the Upper Triassic evaporite ('Calcare Cavernoso' Fm) and the overlying, impermeable, Ligurian and Sub-Ligurian units, which have played a fundamental role in fluid containment (Dessau *et al.* 1972;

https://doi.org/10.1017/S0016756822001200 Published online by Cambridge University Press

Tanelli, 1983; Tanelli & Scarsella, 1990; Tanelli *et al.* 1991; Lattanzi, 1999); (4) they are characterized by silicic (jasperoid) and, subordinately, argillic alteration (Tanelli & Scarsella, 1990; Tanelli *et al.* 1991).

The Sb-ore bodies were intensively exploited during the first half of the nineteenth century when at least 17 mines were active (Campiglia, Capita, Casal di Pari, Cetine, Macchia-Casella, Manciano, Montauto, Monticchio, Niccioleta, Pereta, Pietrarotonda–Salamagna, Poggio Fuoco, Rosia, San Martino sul Fiora, Selvena, Tafone, Zolfiere; list provided by Morteani *et al.* 2017). The deposition is still ongoing as testified to by the stibnite and metastibnite precipitation observed some years ago at the Pereta and Tafone mines (Dessau, 1952; Klemm & Neumann, 1984), as well as by the Sb- and As-rich geothermal fluids (0.2–1.3 mg/L Sb and 22.5–65.4 mg/L As) and the Sb-rich (75 %) scales in the wells (Morteani *et al.* 2017) and piping (Cappetti *et al.* 1995; Möller *et al.* 2009; Morteani *et al.* 2011) of the Piancastagnaio geothermal field and power plant, respectively.

The Sb-mineralization of Poggio Peloso hill was first documented by Rimbotti (1884) but never exploited due to its low industrial potential (Brizzi & Sabelli, 1985). Reported minerals are: quartz, as the main gangue mineral of Sb-bearing minerals, followed by calcite; stibnite (Sb_2S_3), in radial nodules of thin crystals (2–3 cm); stibiconite ($Sb_3O_6(OH)$), often pseudomorphic on stibnite; valentinite (Sb_2O_3), generally in spherules with a radius of a few millimetres; rare senarmontite (Sb_2O_3), showing small colourless octahedra; very rare onoratoite ($Sb_8O_{11}Cl_2$); pyrolusite (MnO_2), in the form of concretions of blackish powder; alunite ($KAl_3(SO_4)_2(OH)_6$), generally present as a white powder often associated with stibiconite; frequent barite ($BaSO_4$), in tabular crystals typically below centimetre size; and Fe-hydroxides (Braga, 1980; Brizzi & Sabelli, 1985).

Brogi & Fulignati (2012) described the Pietratonda–Poggio Peloso Sb-mineralization as 'a fossil hydrothermal system that was probably active during the volcanic activity that produced rhyolitic lava flows' of the neighbouring Roccastrada volcanic complex (~2.3 Ma). What was the source of the Sb is still a matter of debate. Dessau *et al.* (1972) suggested that the metals had either a magmatic origin (direct) or that they were leached from the rocks crossed by the fluids (indirect). Lattanzi (1999) suggested the existence of a distal 'magmatic connection' with the igneous rocks of the 'Tuscan Magmatic Province', even in the absence of a physical contact between the mineralization and the igneous bodies. On this basis, Brogi & Fulignati (2012) speculated on the existence of a similar 'magmatic connection' between the Sb-deposits of Poggio Peloso and the Roccastrada volcanic complex.

Gold occurrences have long been associated with Sb- and Ba-deposits (Tanelli *et al.* 1991), and 'disseminated' gold has been found in this ore deposit (Pipino, 1988; Tanelli & Scarsella, 1990; Tanelli *et al.* 1991; Lattanzi, 1999). Lattanzi (1999) hypothesized that the igneous rocks of the Tuscan Magmatic Province may have been likely gold contributors, as well as the ophiolites of the Ligurian units as suggested by Montini *et al.* (1995). The latter found a positive Au–Cr correlation in mineralized samples at Frassine (Monterotondo Marittimo, Grosseto) and observed that the only likely source of Cr in the area was the ophiolites occurring in the Ligurian units.

3. Materials

The list of investigated samples is provided in Table 1 and sampling sites are shown in Figure 1.

Six samples of chalcedonies were collected at Poggio Peloso (Fig. 2). All the chalcedonies showed the typical light blue colour, alternating to lighter (up to whitish) or darker (up to greyish) bands. Only sample PP5 showed light orange to light grey/blue bands. The hand specimens showed primary crustiform and colloform textures, while zonal marking was only present in sample PP5. Banding was generally parallel to the rim. Overall, these agates can be described as wall-lining and vein agates. The host rock was the Calcare Cavernoso (Triassic evaporitic Burano Fm) for all samples.

Considering the various hypotheses formulated on the origin of antimony and gold, it was immediately clear that a sampling exclusively focused on chalcedonies would not have provided convincing answers. Therefore, samples of the carbonate base of the Tuscan Nappe (sample V9), the underlying Verrucano Group (samples V1–V3), the Upper Triassic evaporites (samples V4, V5) and the Palaeozoic phyllites (samples V6–V8) were also collected with the aim of determining their trace compositions. In addition, two samples of Palaeozoic metamorphic rocks drilled in the Monte Amiata geothermal area, consisting of graphitic quartz-metasandstone and metasiltite and graphitic phyllite, coming from the geothermal wells BG3bis (sample A2) and BG25 (sample A1), at depths of 3111 and 3663 m below the ground level, respectively, were also analysed for comparison. Sample A2 was collected in correspondence with a fractured volume (Ruggieri *et al.* 2004) hosting the deeper (2500–3500 m below ground level) exploited geothermal reservoir (Batini *et al.* 2003; Bertini *et al.* 2005).

4. Methods

4.a. LA-ICP-MS

LA-ICP-MS measurements were performed on flat-polished samples. The instrument combines an ablation microbeam based on a Nd:YAG laser source (Brilliant, Quantel) operating at 266 nm (for details see Tiepolo *et al.* 2003) and a quadrupole ICP-MS (PerkinElmer Sciex-Elan DRC-e). Thirty-four masses from ^{7}Li to ^{238}U were acquired; the laser was operated at a 10 Hz repetition rate, the power on the sample was 1.5 mW and the spot size was set at 50 µm. The optimization of the LA-ICP-MS to minimize elemental fractionation was performed by ablating NIST 610 glass and adjusting the nebulizer Ar and the carrier laser cell He gas flows to obtain the ratio of ^{232}Th and ^{238}U signals close to 1 by minimizing the ThO+/Th+ ratio (<1 %) in order to reduce the formation of polyatomic oxides. Accuracy was assessed on the USGS BCR-2 reference glass (analysed as an unknown in each analytical run) and was better than 20 % at the sub parts per minute (ppm) level. Data reduction was carried out with the software package GLITTER (van Achterbergh *et al.* 2001) and using NIST SRM 610 and ^{29}Si as external and internal standards, respectively.

4.b. X-ray fluorescence

Major and minor element compositions of the bulk rocks were determined by XRF. Samples were mechanically crushed in a planetary mill and manually ground into a powder in an agate mortar. Quantitative analyses were performed on powder discs obtained by pressing 0.5 g of sample on a support of boric acid. The XRF instrument was a Philips MagiX-Pro. Background and mass absorption intensities were calculated using calibrations based on 24 international geological reference materials. Loss on ignition was determined by heating samples to 1050 °C for 2 hours.

https://doi.org/10.1017/S0016756822001200 Published online by Cambridge University Press

Table 1. Rock samples list

Sample no.	Rock type	Sampling site	Unit	Main (and minor) mineralogical phases	Age
V9	Dolostone	Pietratonda–Paganico	Evaporite (Burano Fm, Tuscan Nappe)	Dol (+ Cal, Qz)	Retico
V1	Quartz-metaconglomerate	Monte Leoni	Metasiliciclastic rocks (Verrucano Group, Monticiano Roccastrada Unit)	Qz + wm (+ Chl, Opq)	Trias
V2	Metasiltstone	Monte Leoni	Metasiliciclastic rocks (Verrucano Group, Monticiano Roccastrada Unit)	Qz + wm + Chl (+ Fsp, Opq)	Trias
V3	Quartz-metasandstone	Monte Leoni	Metasiliciclastic rocks (Verrucano Group, Monticiano Roccastrada Unit)	Qz + wm + Chl (+ Fsp, Opq)	Trias
V4	Dolostone	Roccastrada	Evaporite (Burano Fm, Tuscan Nappe)	Dol + Gp (+ Cal)	Late Triassic
V5	Gypsum	Roccastrada	Evaporite (Burano Fm, Tuscan Nappe)	Gp (+ Dol)	Late Triassic
V6	Quartz-metasandstone	Civitella	Palaeozoic metasiliciclastic rocks (Phyllite-quartzitic Group, Farma Fm)	Qz + wm (+ Fsp, sul, Opq)	Late Palaeozoic
V7	Quartz-metasandstone and metasiltite	Civitella	Palaeozoic metasiliciclastic rocks (Phyllite-quartzitic Group, Farma Fm)	Qz + wm (+ Fsp, sul, Opq)	Late Palaeozoic
V8	Graphitic metasiltite	Civitella	Palaeozoic metasiliciclastic rocks (Phyllite-quartzitic Group, Farma Fm)	Qz + wm (+ Fsp, sul, Opq)	Late Palaeozoic
A1	Graphitic metasiltite	BG25 well	Palaeozoic metasiliciclastic rocks (Phyllite-quartzitic Group, Farma Fm)	Qz + wm (+ Cal, Opq)	Late Palaeozoic
A2	Quartz-metasandstone and metasiltite, graphitic phyllite	BG3bis well	Palaeozoic metasiliciclastic rocks (Phyllite-quartzitic Group, Farma Fm)	Qz + wm + Chl (+ Cal, Opq)	Late Palaeozoic

Abbreviations: Qz – quartz; wm – white mica; Chl – chlorite group; Cal – calcite; Dol – dolomite; Fsp – feldspars; Gp – gypsum; Opq – opaque minerals such as Fe- and Ti-oxides; sul – sulfates of the alunite-jarosite group. Further information on the mineralogical assemblage is provided in online Supplementary Material Note 1.

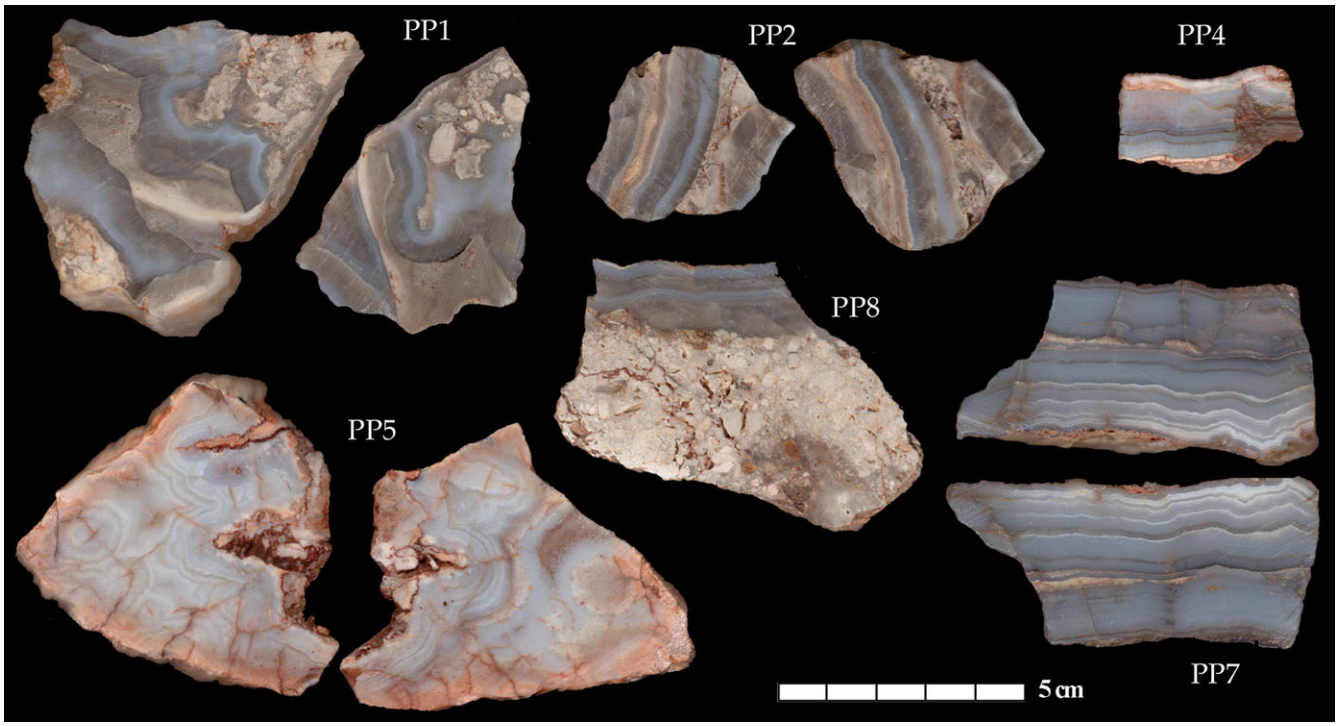

Fig. 2. (Colour online) The chalcedonies from Poggio Peloso investigated in this study.

https://doi.org/10.1017/S0016756822001200 Published online by Cambridge University Press

4.c. Optical microscopy

All chalcedonies were cut orthogonally to the banding and polished. Half of the polished sample was prepared in thin-section for optical microscopy (OM) observations, while the other opposite half was investigated by LA-ICP-MS. Rock sample nos V1–V9 were prepared in thin-section to evaluate the possible presence of microfeatures that could lead to their exclusion and to decide the points on which to conduct further analyses.

4.d. Powder X-ray diffraction

An aliquot of ~20 g was crushed and pulverized in an agate mortar. About 1 g was used for powder X-ray diffraction (PXRD), carried out on an automated PANalytical X'Pert PRO diffractometer, using Cu–Ka radiation (Ni-filter, 2θ range = 5–70°, step size = 0.02°, time per step = 1 s, room temperature = 25 °C). Measurements were performed on powders gently pressed into a back-loading cavity mount. The phase analysis was carried out using the software X'Pert HighScore Plus that uses the Inorganic Crystal Structure Database (ICSD). The starting coordinates of the atoms, cell parameters and space groups were taken from Le Page & Donnay (1976) for quartz, Brigatti *et al.* (1998) for phengitic muscovite, Walker & Bish (1992) and Guggenheim & Nelson (1993) for clinochlore, Kawano *et al.* (1998) for sericite, Aleksandrova *et al.* (1973) for sudoite, Neder *et al.* (1999) for kaolinite, Cole *et al.* (1949) for sanidine, Chao *et al.* (1940) for orthoclase and Ferguson *et al.* (1958) for albite.

5. Results

5.a. The chalcedonies

5.a.1. LA-ICP-MS

The average composition of all samples is characterized by SiO_2 contents ranging from 98.0 to 99.8 wt % (av. 99.1 wt % ± 0.3) and a rather low minor- and trace-element content, i.e. the typical composition of chalcedonies and agates (see, e.g. Blankenburg, 1988; Tanaka & Kamioka, 1994; Merino *et al.* 1995; Götze *et al.* 2001; Möckel & Götze, 2007; Götze *et al.* 2009, 2016). Some spots with low SiO_2 and high Ca, Mg, Al, K or Fe contents were also identified as carbonates, feldspars and metal oxide inclusions. The presence of inclusions made it necessary to exclude some measurements (fully provided in the online Supplementary Material Tables S1–S6 and Figs S1–S6) from the calculation of the average composition of the chalcedonies provided in Table 2. Table 2 shows that SiO_2 contents of the chalcedony range between 99.2 and 99.4 wt % and that none of the other minor and trace components is above 1000 ppm, except for Sb. The latter show contents (1543–1846 ppm; average 1697 ± 119 ppm) that greatly exceed those reported for the upper continental crust (UCC) (0.4 ppm; Rudnick & Gao, 2003) or for surficial waters (<0.001 ppm) (Filella *et al.* 2007). To a lesser extent, B and Ge are also enriched, ranging on average between 81 and 113 ppm for the former and between 7 and 9 ppm for the latter. As for Ba contents, it is worth underlining that the amounts reported in Table 2 are underestimated. Indeed, numerous Ba-rich inclusions were found but omitted from the calculation of the average chalcedony composition.

The correlations between elements and element pairs are shown in online Supplementary Material Figures S1–S6 and Tables S7–S12, respectively. Here the attention is focused on the correlation coefficients of Sb with major, minor and trace elements (Table 3) and on correlated pairs of elements (Table 4). Sb can be strongly correlated ($r > 0.9$) with B, Mn, As and Cs or well correlated ($0.60 < r < 0.89$) to poorly correlated ($0.40 < r < 0.59$) with all the remaining elements. The correlation with B and, to a lesser extent, Mn, As and Cs appears consistent among the different samples (Table 3; Fig. 3). On the contrary, the correlation with the other elements is only observed in a few samples. The well to strongly correlated pairs Be–Mn, Be–Ga, B–Rb, K–Rb, K–Cs, Rb–Cs and Ba–Sr, and the poorly correlated pair SiO_2–Ge are worth noting (Table 4).

As for gold, despite that the values are to be considered qualitative, this element has been frequently detected, both in chalcedony and carbonate inclusions. The significance of its correlation is lowered by the small number of available measurements but appears consistent with Ag in sample PP7 ($r = 0.865$). As for the correlation between chromophores and agate colours, the techniques used are not suitable for proposing conclusive information. For example, (a) the variability of Fe and Mn amounts cannot be correlated to light/dark bands in the geochemical profiles of samples PP1, PP2, PP5, PP7 and PP8, and (b) the whitish and blue bands of sample PP4 show comparable contents of both Fe and Mn. Conversely, the brown band of the latter sample (online Supplementary Material Table S3, measurement no. 11) shows the highest Fe and Mn values.

As for REE contents, the chalcedonies show a depleted chondrite-normalized pattern (Fig. 4a), which is typical of these materials. Except for PP7 showing a La_n/Lu_n ratio below 1, light REEs (LREEs) prevail over heavy REEs (HREEs) in the other samples (La_n/Lu_n ratio 1.3–4.2). The LREE normalized patterns show a decreasing slope in all samples (La_n/Sm_n 1.3–5.2) except PP5 (La_n/Sm_n 0.6). A slight negative Ce anomaly is present in all samples (Ce/Ce* 0.57–0.94), except PP5 and PP7 for which it cannot be determined. Conversely, a weak to strong positive Eu anomaly characterizes all samples (Eu/Eu* 1.67–6.32). The HREE normalized patterns show an increasing slope (Gd_n/Lu_n 0.4–0.6), except in PP1 and PP5 (Gd_n/Lu_n 1.2 and 2.3, respectively). The UCC-normalized REE pattern (Fig. 4b) is particularly depleted and shows an enrichment of HREEs with respect to LREEs. Both La_n/Lu_n and Gd_n/Lu_n ratios are constantly below 1 (range 0.06–0.76), as shown by the overall increasing slope of the patterns. The Ce anomaly is negative in all samples (Ce/Ce* 0.20–0.95) except PP4 (Ce/Ce* 2.05), while the Eu anomaly is always positive (Eu/Eu* 1.03–7.28).

5.a.2 . PXRD

Quartz was identified in all samples. Calcite has been clearly detected in sample PP2 while barite and haematite were rarely detected. The results of the XRD analyses performed on the rocks analysed for comparison are provided in the online Supplementary Material (Note 1) and confirmed the macroscopic identification of the sampled rocks.

5.a.3. Optical microscopy

The samples are mainly constituted by fibrous chalcedony (length-fast) and micro-/macro-crystalline quartz. In the following description, the correspondence with the spot-analyses (i.e. 'S(no.)-no./nos') refers to LA-ICP-MS measurements (online Supplementary Material Tables S1–S6). In sample PP1, long fibres of fan-shaped chalcedony with flamboyant extinction (S1- nos 14, 15) are richer in Mg, V, Mn, B, Na, K, Cs, As and Rb, and lower in Be, Al and Cu with respect to the thin parallel-bladed fibres (S1-nos 10, 11). Sb, Sr, Ba and Ga contents are similar in both types of

https://doi.org/10.1017/S0016756822001200 Published online by Cambridge University Press

Table 2. LA-ICP-MS data. The chemical composition of the chalcedony. Average values provided as ppm if not differently specified. Measurements of quartz and inclusions were omitted from calculation

Sample	PP1		PP2		PP4		PP5		PP7		PP8		Total	
	$n = 7$	SD	$n = 6$	SD	$n = 7$	SD	$n = 7$	SD	$n = 15$	SD	$n = 6$	SD	$n = 48$	
SiO_2 (wt%)	99.25	0.10	99.18	0.01	99.20	0.05	99.28	0.07	99.37	0.13	99.23	0.11	99.25	0.07
Be	21.8	4.3	29.7	18.9	47.8	26.8	28.7	10.1	26.6	17.4	37.9	13.0	32.1	9.3
B	112.7	24.7	112.0	17.6	98.6	12.8	102.4	14.9	81.1	19.5	99.8	11.8	101.1	11.5
Na	108.3	51.9	127.5	49.0	71.8	13.4	104.1	20.8	125.6	28.4	69.6	7.1	101.1	25.3
Mg	20.6	12.9	18.2	11.3	12.0	2.3	21.0	7.2	19.6	9.6	28.9	27.7	20.0	5.5
Al	20.1	9.2	25.1	12.7	44.1	19.3	39.6	19.1	42.2	20.1	50.0	25.7	36.8	11.7
K	122.8	32.0	125.2	24.9	135.1	18.0	138.7	28.7	114.5	29.5	128.1	18.8	127.4	8.7
Ca	511.4	286.8	621.8	–	227.8	83.5	205.7	–	475.8	107.9	363.0	113.8	400.9	165.0
Ti	3.0	3.4	4.8	2.7	0.6	0.0	6.1	0.2	6.0	1.6	7.9	10.2	4.7	2.6
Mn	323.7	98.7	414.6	65.3	618.2	158.8	655.1	97.5	574.7	215.8	488.6	51.8	510.3	126.2
Fe	31.7	18.0	49.9	28.8	56.0	45.2	94.8	71.8	30.9	14.2	75.9	36.8	56.5	25.1
Ga	0.6	0.3	1.9	1.7	4.4	2.6	2.1	1.5	2.5	2.7	2.1	1.3	2.3	1.2
Ge	6.9	0.6	9.2	1.1	8.6	1.7	8.5	0.9	9.4	1.3	8.1	1.0	8.5	0.9
As	10.2	1.8	9.2	1.5	8.4	1.5	11.0	1.9	9.4	2.2	8.6	1.2	9.5	1.0
Rb	0.9	0.3	1.0	0.2	0.8	0.2	1.1	0.3	0.9	0.3	0.8	0.1	0.9	0.1
Sr	2.5	1.5	4.6	1.3	6.7	1.3	4.8	1.0	3.4	1.4	9.5	12.6	5.2	2.5
Sb	1846	198	1577	68	1737	82	1788	145	1690	279	1543	112	1697	119
Cs	0.6	0.1	0.6	0.1	0.5	0.1	0.5	–	0.4	0.1	0.5	0.1	0.5	0.1
Ba	8	14	31	23	81	28	28	13	14	13	34	25	33	26
La	0.287	0.066	0.343	0.136	0.163	0.047	0.049	0.020	0.099	0.082	0.425	0.092	0.228	0.147
Ce	0.364	0.146	0.284	0.217	0.249	0.174	0.049	0.029	0.070	0.043	0.446	0.207	0.244	0.158
Pr	0.036	0.027	0.018	–	0.016	0.002	–	–	–	–	0.014	0.005	0.021	0.010
Nd	0.144	0.084	0.147	0.055	0.103	0.017	0.058	0.048	0.066	0.057	0.115	0.055	0.106	0.038
Sm	0.059	0.007	0.043	0.012	0.065	0.067	0.050	0.012	0.048	0.035	0.051	–	0.053	0.008
Eu	0.047	0.017	0.069	0.025	0.034	0.017	0.089	–	0.099	0.032	0.095	0.039	0.072	0.027
Gd	0.070	0.005	0.043	0.014	0.057	0.016	0.070	0.041	0.070	0.049	0.038	0.028	0.058	0.015
Tb	0.008	0.005	–	–	0.011	0.000	0.016	–	0.014	–	0.006	0.004	0.011	0.004
Dy	0.041	0.012	0.044	–	0.029	0.014	0.038	0.018	0.055	–	0.025	0.008	0.039	0.011
Ho	0.010	0.002	0.011	–	0.008	0.004	–	–	–	–	0.008	–	0.009	0.001
Er	0.016	0.001	0.027	0.016	0.030	0.027	0.040	0.018	0.035	–	–	–	0.030	0.009
Tm	–	–	0.012	–	0.008	0.000	0.006	–	–	–	–	–	0.008	0.003
Yb	0.037	0.011	0.056	–	–	–	0.042	–	0.045	0.016	0.093	–	0.055	0.022
Lu	0.007	0.003	0.010	0.008	0.012	0.011	0.004	0.001	0.016	0.011	0.012	0.011	0.010	0.004

textures. In sample PP2, the sequence includes several textures: fibrous flamboyant (S2-nos 1–4), comb, parallel-bladed (S2-nos 9, 10 and 13–15) and pseudo-granular (S2-nos 1, 11, 12, 16, 17). The last band of granular quartz (S2-nos 22, 23) contains the highest SiO_2 and the lowest levels of almost all other elements, except for Mg, Ca and As. A thick and heterogeneous layer mainly constituted by calcite (S2-nos 5–8) is also present. Sample PP4 shows several generations of hatched bands ('Runzelbänderung'), constituted by long and thin parallel fibres, alternating with thin layers of comb quartz. In sample PP5, the pseudo-granular texture (S4-nos 3, 4, 7–17) is generally poorer in most elements with respect to the flamboyant spherulites and fan-shaped fibres (S4-nos 1, 2, 5, 6). In sample PP7, the chemical composition varies without an apparent consistency among the different depositional layers. The layers show flamboyant (S5-nos 1, 2, 15–17, 22–27), parallel-bladed (S5-nos 3–8, 20–21) and feathery chalcedony (S5-nos 13, 18), along with comb (S5-nos. 14, 19) and granular quartz (S5-nos 9–12, 28, 29). Similarly, to the previous sample, PP8 also shows parallel-bladed (S6-nos 1, 2, 5, 6), flamboyant (S6-nos 3, 4, 7) fibres along with comb micro- and macro-quartz (S6-nos 8–10). The last layer is constituted by granular quartz and abundant residues of carbonaceous materials (S6-nos. 11, 12).

Regarding the distribution of the elements in the various layers, it may be interesting to note that while the antimony remains at almost comparable levels in all types of textures and generally decreases drastically in correspondence with carbonate inclusions, gold is present in chalcedony and carbonates while absent in comb quartz. A series of photos of the main textures (with a scale of detail greater than those given in the online Supplementary Material) is provided in Figure 5.

5.b. The rocks

The rocks were analysed only to confirm their identification and to estimate their Sb and Au contents; however, a complete analysis is provided for most of them in the online Supplementary Material (Note 1; Table S13).

The rocks are characterized by low to very low amounts of Sb: below 1 ppm in samples V1, V4, V5, V6, V7, V9 and R; between 1 and 2 ppm in samples V3, V8 and A1; and between 3 and 4 ppm in samples V2 and A2. Among the other elements, while minor and trace elements typically show higher values in the rocks than in the chalcedonies, the contents of Be and Ge appear systematically higher in the chalcedonies. The relatively high contents of B in samples V9 and A2, Mn in samples V9, A1 and A2, as well as the amounts of Au measured in samples V1, V7–V9, A2 and, especially, A1 may be informative for comparison.

Figure 4c shows the REE patterns of the examined rock samples and those of the Palaeozoic phyllites from the Larderello–Travale geothermal area analysed by Möller *et al.* (2009). The first observation to make is that none of the rock samples show such pronounced depletion as that observed in the chalcedonies except V1. The Ciabattino and Boccheggiano samples appear particularly enriched compared to those investigated in this study, while the Radicondoli sample is comparable with both V6 and V7. The general trend of the phyllites is decreasing except in samples A1 and A2, which also show an increase in HREEs compared to LREEs. The different pattern of these two samples compared to the other rocks is probably due both to the partially different mineralogy (including the relative abundance of the accessory phases) and to the different migration speed of the HREEs compared to the LREEs in different conditions of alteration (in particular pH variability). As they fall beyond the scope of this research, we will not dwell on these aspects, while it is worth noting another important feature concerning the Eu anomalies. While the samples A1, A2 and V3 show a weak positive Eu anomaly (similar to the chalcedonies), the phyllites analysed by Möller *et al.* (2003, 2009) and the other metamorphic rocks investigated here are characterized by a negative Eu anomaly (Eu/Eu* 0.5–0.9). Furthermore, the samples A1 and A2 show a La_n/Lu_n ratio (0.8–1.2) closest to that of the chalcedonies.

In Figure 4d, the REE patterns of the chalcedonies are further compared with those of the Tuscan volcanites. The data obtained by Giraud *et al.* (1986) and Pinarelli *et al.* (1989) on the volcanites from both Roccastrada and Monte Amiata evidence a clear difference not simply related to the absolute REE contents but also regarding the overall behaviour of the REEs.

6. Discussion

6.a. Poggio Peloso chalcedony: an outlier based on Sb contents

The samples from Poggio Peloso contain the highest Sb amounts found so far in chalcedonies. Table 5 shows a selection of reference data including chalcedony, carnelian and agate, as well as quartz, amethyst, chert/flint, jasper and quartzites from several locations. Low amounts of Sb are typically found in all silica-based minerals and rocks; however, the contents measured by the authors in agates rarely exceed 50 ppm.

Therefore, the comparison describes the chalcedonies of Poggio Peloso as 'outliers' with respect to Sb amounts, precisely as the high contents of Zr (between 295 and 687 ppm) found in vein agates from 'Borówno' quarry (Lower Silesia) distinguished the Polish samples (Powolny *et al.* 2019).

6.b. Positive Eu anomaly: hydrothermal environment

Comparing the REE patterns provided by Morteani *et al.* (2017) for calcite with those obtained for the Poggio Peloso chalcedony, a striking difference emerges regarding Eu anomalies. While calcite patterns are characterized by negative Eu anomalies, the chalcedonies show positive anomalies. This result represents an anomalous feature even for chalcedonies, and it has been rarely observed (e.g. in vein and moss agates from the 'Borówno' quarry in Poland; Powolny *et al.* 2019).

As for calcite, Morteani *et al.* (2017) explained the negative anomaly due to the poor Eu^{2+} uptake capacity of Ca minerals, based on the thermochemical reduction of Eu^{3+} to Eu^{2+} by high-temperature deep-seated aquifers. As regards the chalcedonies, it should be remembered that Eu^{2+} is present in a variety of magmatic and hydrothermal environments while it is rare in sedimentary environments because it is linked to particularly reducing conditions (Brookins, 1989). In aqueous solutions, the redox potential of Eu/Eu* is affected by temperature and, to a lesser extent, by pH, pressure and REE speciation (Bau, 1991). As a consequence, positive anomalies such as those observed in the chalcedonies are found in acidic, reducing hydrothermal fluids and sediments in an active ridge system (Kamber & Webb, 2001; Michard *et al.* 1983; Michard, 1989; German *et al.* 1990). Furthermore, Eu enrichment may also reflect plagioclase weathering since Eu substitutes into the calcium site of plagioclases (see, e.g. Cabioch *et al.* 2006). However, Eu^{2+} can also substitute Ba^{2+} (Shannon, 1976; Guichard *et al.* 1979; Mazumdar *et al.* 1999), thus making barite a possible carrier phase. In chalcedonies,

https://doi.org/10.1017/S0016756822001200 Published online by Cambridge University Press

Table 3. Correlation coefficients (*r*) of Sb with major, minor and trace elements in the chalcedonies (LA-ICP-MS data)

	SiO_2	Li	Be	B	Na	Mg	Al	K	Ca	Sc	Ti
PP1	−0.523	0.111	0.555	0.559	0.298	0.477	0.459	0.670	−0.307	−0.098	0.252
PP2	−0.890	0.493	0.291	0.846	0.851	−0.417	−0.367	0.892	0.004	0.900	−0.166
PP4	−0.316	0.078	0.115	**0.949**	0.832	0.222	−0.095	0.556	0.081	−0.234	0.298
PP5	−0.186	0.547	−0.424	0.805	0.431	0.404	0.742	−0.500	−0.407	0.693	0.485
PP7	−0.813	−0.121	0.402	**0.910**	0.522	−0.147	0.261	0.693	−0.066	0.084	0.584
PP8	−0.419	0.053	0.486	**0.982**	−0.240	−0.100	0.661	−0.550	−0.055	0.780	0.178
	V	Cr	Mn	Fe	Co	Ni	Cu	Zn	Ga	Ge	As
PP1	0.244	–	0.289	0.484	0.305	0.344	0.036	0.341	0.329	0.103	0.884
PP2	0.153	–	0.873	−0.136	−0.348	−0.181	−0.403	0.382	0.401	−0.294	**0.932**
PP4	0.538	–	0.273	0.399	–	−0.110	0.325	0.617	−0.174	0.191	0.856
PP5	−0.500	–	0.669	0.742	0.761	−0.575	−0.059	−0.118	−0.709	0.572	0.728
PP7	−0.132	−0.186	0.703	0.234	−0.532	−0.122	−0.201	0.288	0.245	−0.139	0.700
PP8	−0.055	–	**0.906**	−0.311	−0.383	−0.200	−0.963	0.306	0.322	−0.055	0.577
	Rb	Sr	Y	Zr	Nb	Mo	Ag	Cd	In	Cs	Ba
PP1	0.678	0.872	0.339	0.044	0.737	0.160	0.742	−0.366	−0.551	**0.934**	0.740
PP2	0.670	0.462	−0.224	−0.400	–	–	0.244	0.539	−0.151	0.628	0.258
PP4	0.048	−0.030	–	–	0.243	−0.131	0.261	0.659	−0.393	0.600	−0.191
PP5	−0.007	−0.571	0.414	0.446	0.409	0.448	0.448	–	0.456	0.865	−0.515
PP7	0.714	0.446	0.121	0.324	0.025	−0.281	−0.064	0.209	0.144	0.729	0.082
PP8	0.286	0.227	–	0.878	0.536	−0.890	0.359	–	0.380	0.228	0.200

Highest values are marked in bold.

Table 4. Correlated pairs of elements in the chalcedonies (LA-ICP-MS data)

	SiO_2–Ge	Be–Mn	Be–Ga	B–Rb	K–Rb	K–Cs	Rb–Cs	Ba–Sr
PP1	0.175	−0.196	−0.060	0.783	**0.976**	0.871	0.844	**0.952**
PP2	0.495	0.604	**0.985**	0.792	0.802	0.634	**0.915**	0.868
PP4	0.645	0.888	**0.914**	0.004	0.181	0.158	0.624	0.807
PP5	0.111	0.274	0.570	0.157	−0.445	−0.223	0.064	**0.967**
PP7	0.403	0.760	**0.924**	0.785	0.755	0.771	0.755	0.844
PP8	−0.284	0.781	0.848	0.220	−0.480	−0.646	0.049	**0.999**

Highest values are marked in bold.

barite inclusions are indicative of the activity of SO_4^{2-} in the mineralizing medium, and Ba is one of the elements promoting silica precipitation in alkaline solutions (Dumańska-Słowik *et al.* 2018).

Möller *et al.* (2009) reported the C1-chondrite-normalized patterns of REY in liquid and vapour produced by some wells of the Monte Amiata geothermal field. In particular, the liquid phase is characterized by strong Eu and moderate Y positive anomalies, which were interpreted to be the result of REY fractionation during water–rock interaction in the fluid source region. In particular, the deep fluid productive horizons of the Monte Amiata geothermal field are hosted in the Palaeozoic metamorphic rocks represented by the A1 and A2 samples. It is worth reiterating that such samples, contrary to the other Palaeozoic rocks, are characterized by a weak positive Eu anomaly.

6.c. Silica source and transport and Ge enrichment

The *conditio sine qua non* for the formation of chalcedonies is the availability of silica. Silica commonly derives from the weathering or hydrothermal alteration of silicate minerals (effective process) or from the dissolution of amorphous silica or of quartz (less effective process). As a consequence, chalcedony tends to form mainly in areas affected by thermal springs or in formations rich in weatherable silicates. Landmesser (1984) has shown that diffusion of monomeric silicic acid (H_4SiO_4) is the main mechanism in silica transport, based on numerous considerations including the large size/low velocity of colloidal silica and its clear prevalence under a wide range of pH conditions (1–9). This mechanism excludes the transport of silica via free liquid solution, which would also be difficult to explain compared to the low solubility of silica (Krauskopf, 1956).

https://doi.org/10.1017/S0016756822001200 Published online by Cambridge University Press

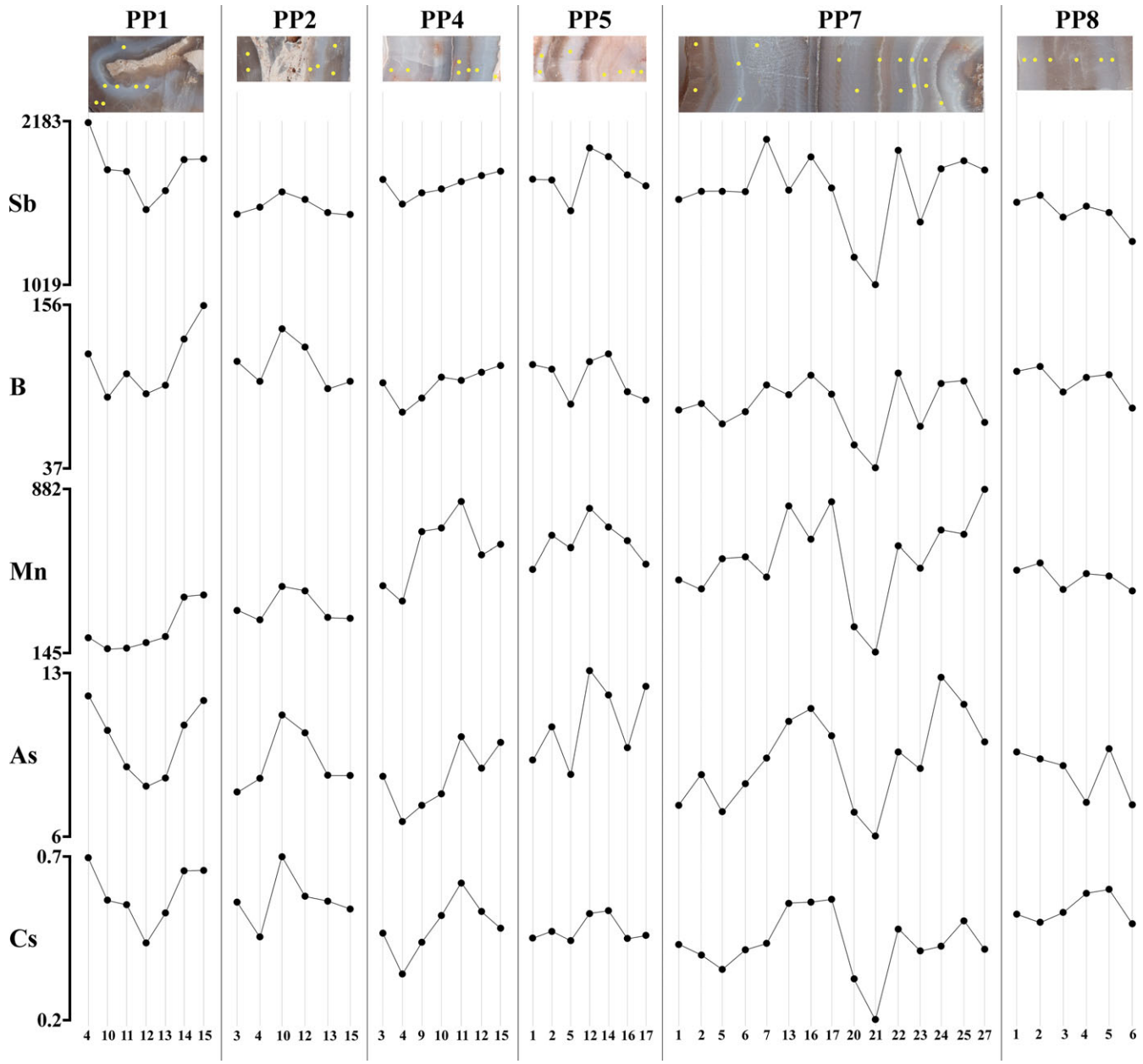

Fig. 3. (Colour online) LA-ICP-MS measurements. The Sb, B, Mn, As and Cs patterns of the chalcedonies from Poggio Peloso.

Considering that the host rocks of the Poggio Peloso chalcedonies are carbonates, the high amounts of silica needed for the formation of chalcedony could have been derived from the volcanic and metamorphic rocks present in the territory or from residual magmatic fluids. Comparing REE contents in the surrounding rocks and chalcedonies, it is evident that the volcanic rocks have such different patterns (Fig. 4d) that it becomes difficult to invoke them as the primary silica source. Most of the metamorphic rocks are overall enriched with respect to the chalcedonies, but their patterns show different LREE and HREE trends (Fig. 4c). As shown above, an interesting analogy with chalcedonies is represented by the weak Eu anomaly shown by the A1–A2 samples from the Monte Amiata geothermal field. It is worth noting that the fluids produced from this geothermal field are characterized by significant concentrations of dissolved silica (up to 1160 ppm; Minissale *et al.* 1997) so that the brines resulting from flashing at the separator are highly supersaturated in silica, causing the formation of silica scales in geothermal pipelines (Vitolo & Cialdella, 1995). Moreover, in one geothermal well, the high silica content is accompanied by significant Sb concentration (up to 50 mg/L), which caused the deposition of SiO_2-rich, stibnite and/or metastibnite-bearing scales in the pipes (Morteani *et al.* 2011). However, the lack of a convincing direct correlation with any of the surrounding rocks suggests that the silica does not derive from the leaching of a unique Si-rich lithology.

The behaviour of Ge in chalcedonies has been frequently related to that of SiO_2, given the similar geochemical behaviour of these two elements and the preferred structural incorporation of Ge in the quartz crystal structure (Götze *et al.* 2009). Ge contents measured in the chalcedonies from Poggio Peloso (7–9 ppm) are higher than those reported for the continental crust (1.4 ppm), lower than those shown by most volcanic agates, while slightly higher than

https://doi.org/10.1017/S0016756822001200 Published online by Cambridge University Press

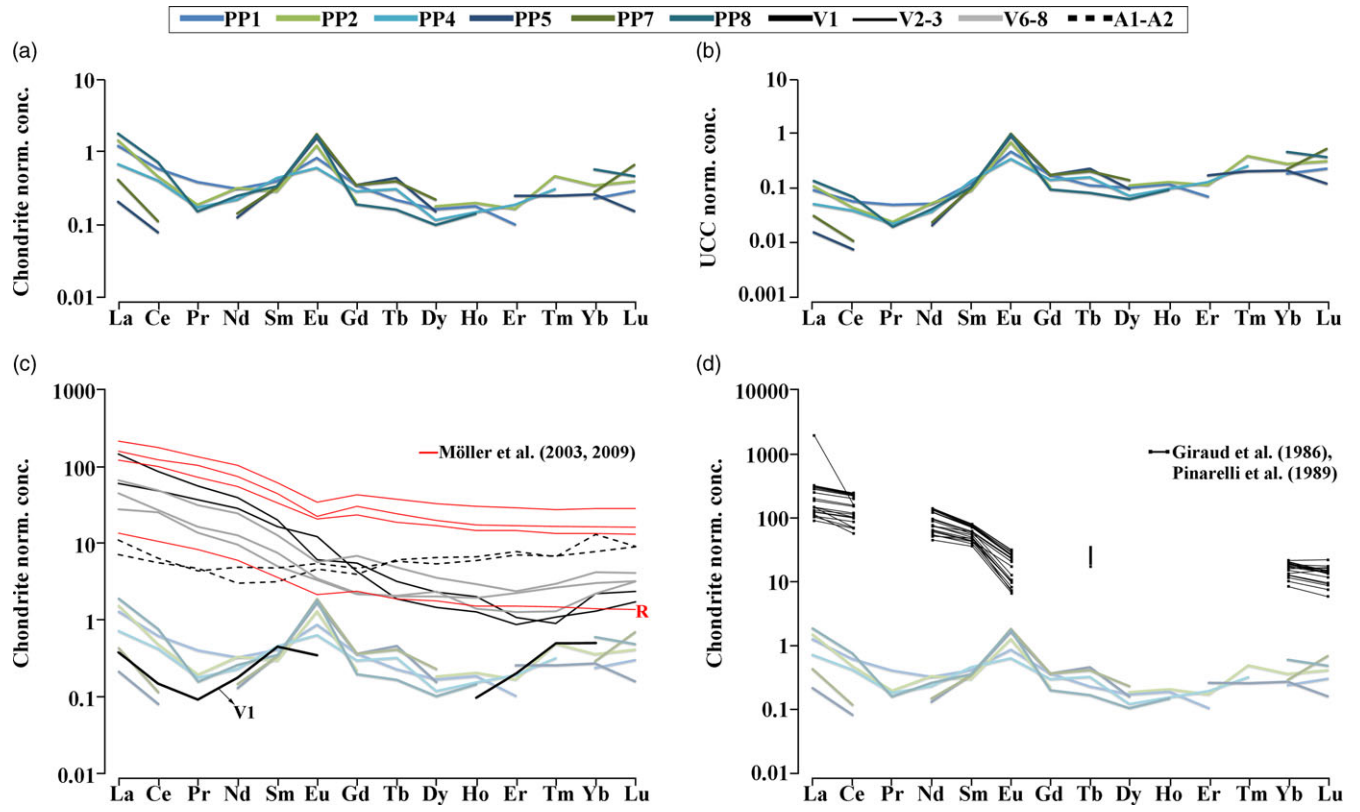

Fig. 4. (Colour online) (a) The chondrite-normalized REE concentration pattern and (b) the upper continental crust (UCC)-normalized trace-element pattern of the chalcedonies (average values from Table 2). (c) The REE patterns of the metamorphic rocks. Black and grey lines indicate the samples investigated in this study. Red lines correspond to the Radicondoli (5.1960 m) drill core chip analysed by Möller *et al.* (2003) – indicated with 'R' – and the phyllites from the well Ciabattino 2 (305 m depth) and the Boccheggiano outcrops (sample nos 10179-B and 10179-D) analysed by Möller *et al.* (2009). For comparison, the pattern of the chalcedonies is visible in the background. (d) REE pattern of selected Tuscanian volcanites compared to the chalcedonies. Reference data from Giraud *et al.* (1986) and Pinarelli *et al.* (1989). The REE concentrations of the chondrite are from McDonough & Sun (1995); those of the UCC are from Rudnick & Gao (2003).

those reported for sedimentary agates (Götze *et al.* 2020; Table 1). As noted in other case studies (e.g. Gliozzo *et al.* 2019), Ge contents are poorly (PP1, 2, 5, 7, 8) to well (PP4) correlated with those of SiO_2; however, the absolute Ge amounts suggest the possible interaction of volatile fluids (HF) and the transport of SiF_4, GeF_4 and BF_3 compounds (for this chemical transport reaction, see Götze *et al.* 2012).

6.d. B, Mn, As and Cs and their correlations with Sb: the fluids

6.d.1. Boron

Contents ranging between 81 and 113 ppm are relatively high, both compared with the crustal B abundance (17 ppm) and the typical range of B content in quartz (from 0 to 25 ppm; Stavrov & Khitrov, 1962), where B^{3+} may replace Si^{4+} in the SiO_4 tetrahedra (see Müller *et al.* 2012 for details on the configuration of trace elements in the quartz lattice).

In magmatic systems, the incompatible behaviour of this lithophile element leads to its strong enrichment in magmatic fluids and vapours as well as in hydrous liquids. Hence, boron enrichment in hydrothermal fluids can derive from magmatic fluids, heating and feeding hydrothermal aquifers with volatile components. However, it can also be influenced by the geochemistry of the local rocks (water–rock interactions; see Bernard-Romero *et al.* 2010) and therefore, being strictly conditioned by the hydrothermal circulation system itself. Among the surrounding rocks, the B-rich Triassic evaporites (Dessau *et al.* 1972) may have represented the most abundant source of B. In this regard, however, it is worth noting that the A2 sample of the Monte Amiata geothermal field also contains remarkable B amounts (191 ppm) and that also the fluids produced by this field are characterized by significant B concentrations (up 3932 ppm; Minissale *et al.* 1997).

6.d.2. Manganese

The correlation of Sb with Mn was unexpected despite the testified presence of concretions of pyrolusite (blackish powder) in the area. Pyrolusite typically occurs in oxidation zones, mainly in sedimentary beds, and in Tuscany, its occurrence is typically related to supergene alteration. In the chalcedonies, manganese contents (324–655 ppm) are lower than those reported for the UCC (0.1 wt %; Rudnick & Gao, 2003). In addition, they are often correlated with Be, which also shows high contents (22–48 ppm) with respect to both the continental crust and the chondrite composition. Be enrichment is frequent in jasperoids (e.g. Johnson, 1977; Lovering & Heyl, 1980; McLemore, 2002, 2010), and beryllium deposits often contain concentrations of manganese oxides together with fluorite, lithium, zinc, uranium and several trace elements (Lindsey, 1977). Consequently, while the observed correlation between Mn and Be is not surprising, it appears more difficult to trace the origin of these two elements. The rocks investigated in this study bear low levels of Mn, except for the carbonates and the A1 and A2 metapelites. Therefore, it seems plausible to hypothesize that the high Mn contents of the chalcedonies mainly derive

https://doi.org/10.1017/S0016756822001200 Published online by Cambridge University Press

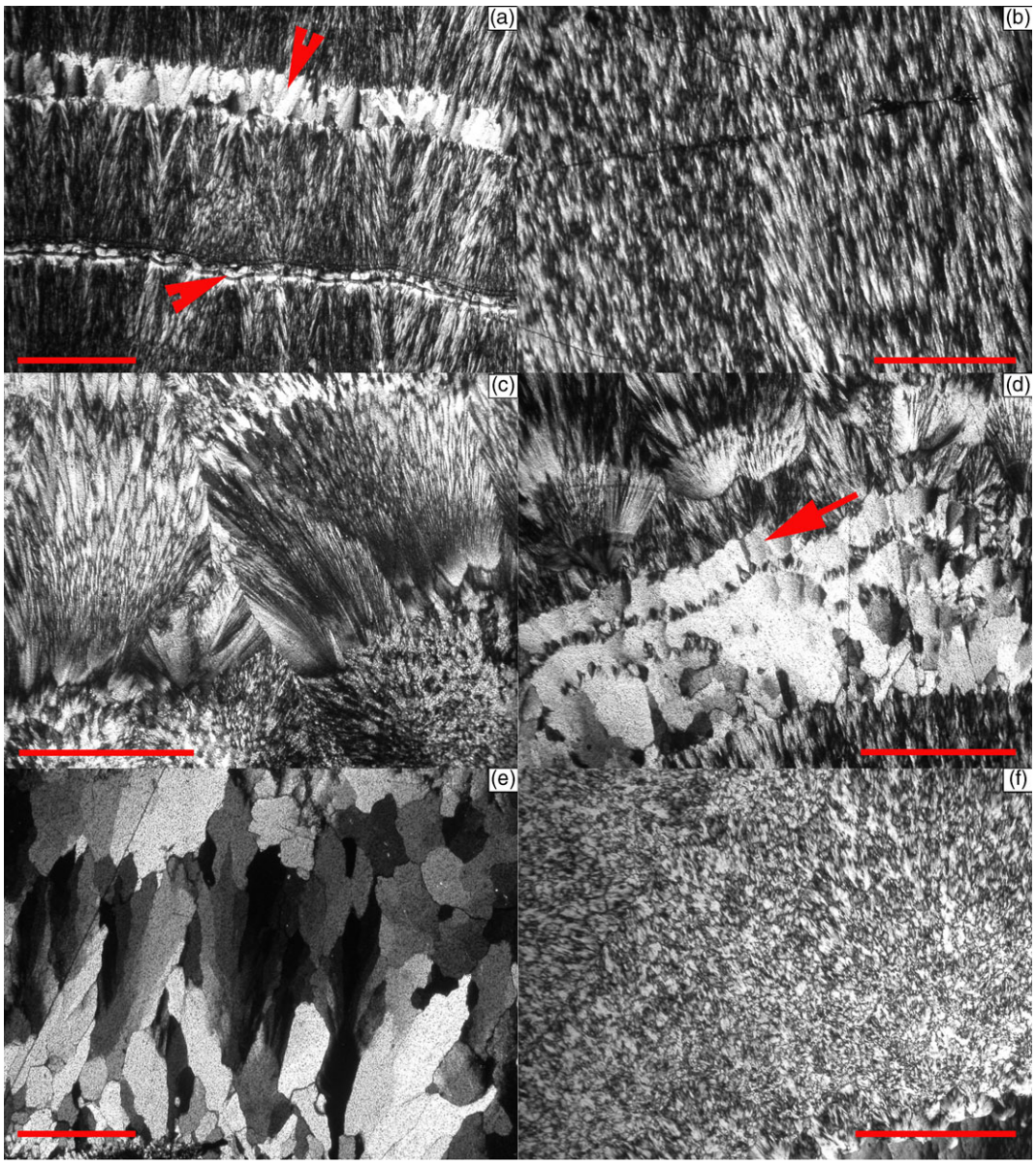

Fig. 5. (Colour online) The textures of chalcedony. OM images (crossed polarized light). (a) Parallel-bladed and comb textures. The arrows indicate two distinct layers of comb quartz. Along the lower one, a concentration of iron oxides approximately corresponds to the dark line indicated by the arrow. (b) Parallel-bladed texture. (c) Flamboyant texture. (d) Flamboyant and comb (indicated by the arrow). (e) Feathery quartz (jigsaw-puzzle texture). (f) Pseudo-granular. The scale bar equals 1 mm.

from the leaching of underlying carbonates. As regards Be enrichment, none of the surrounding rocks shows high levels of this element. However, no data are available on Be amounts contained by the Roccastrada rhyolites, which, in turn, could represent likely candidates. The conduits provided by faults should have then allowed beryllium to circulate, and a wall-rock reaction may have been essential for mineralization processes.

A not compelling but useful example to remember in this regard is the one offered by Lindsey (1977) for Spor Mountains and Honeycomb Hills (Utah). That is to say, carbonate-hosted beryllium (replacement) deposits genetically related to rhyolites (the only ones to return Mn-rich red beryl) and associated with hydrothermal silica, carbonates and other minerals. Moreover, it can be worth remembering that Be-bearing minerals such as bertrandite mainly occur in carbonate replacement deposits such as the jasperoids.

6.d.3. Arsenic

Arsenic enrichment has been frequently used to trace either epithermal gold mineralization (Henley, 1985; Berger & Silberman, 1985; Silberman & Berger, 1985) or geothermal activity (Bingqiu *et. al.* 1986). Geothermal waters and sinters frequently bear high amounts of As, besides Sb and Hg (Weissberg, 1969; Boyle & Jonasson, 1973). Furthermore, this element can be concentrated in hydrothermally altered metasediments (see, e.g. Codeço *et al.* 2021) and in surficial conditions. In the latter environment, As may be released by Fe-hydroxides under oxidizing acid conditions which, in turn, can be obtained owing to sulfide decomposition (see e.g. Craw *et al.* 2000). In the investigated rocks, the highest concentrations of As (17–43 ppm) were measured in the metamorphic rocks (samples V2, V6 and V8). Consequently, the As in the chalcedonies may have been derived from magmatic/hydrothermal fluids and As-enriched meteoric waters.

https://doi.org/10.1017/S0016756822001200 Published online by Cambridge University Press

Table 5. Sb amounts in silica-based minerals and rocks

Type	Country	Locality	N	Min	Max	Av.	SD	Reference
Agate	Afghanistan	–	15	0.06	1.47	0.46	0.4	Law *et al.* (2012)
Chalcedony	Belize	Crooked tree	1	0.7				Cackler *et al.* (1999)
Agate	Brazil	Rio Grande do Sul	1	0.4				*Fallick *et al.* (1987)
Agate	Canada	Agate Island	2	0.3	0.4	0.35	0.1	*McCrank *et al.* (1981)
Agate	Canada	Agate Point	2	0.2	0.2	0.2	–	*McCrank *et al.* (1981)
Chert	China	Yangtze plate	17	3.30	16.70	9.68	4.8	Peng *et al.* (2000)
Agate	Czech Rep.	Frýdštejn, Bohemia	2	2.3	3.0	2.65	0.5	*Beer (1992)
Agate	Czech Rep.	Nova Paka, Bohemia	4	0.20	0.40	0.33	0.1	*Beer (1992)
Flint	Denmark	–	7	0.04	0.10	0.06	–	Olofsson & Rodushkin (2011)
Chalcedony	France	Northern Massif Central	57	10.00	260.00	91.32	58.9	Marcoux *et al.* (2004)
Agate	Germany	Gröppendorf	2	0.2	0.3	0.25	0.1	*Blankenburg (1988)
Quartz	Germany	Gröppendorf	1	0.5				*Blankenburg (1988)
Agate (vein)	Germany	Halsbach	2	3	20	11.5	12.0	*Blankenburg (1988)
Quartz	Germany	Halsbach	1	5				*Blankenburg (1988)
Agate	Germany	Idar–Oberstein	2	4.70	5.20	4.95	0.4	*Schmitt-Riegraf (1996)
Amethyst	Germany	Lauterbach	1	0.2				*Haake & Holzhey (1989)
Quartz	Germany	Lauterbach	1	0.4				*Haake & Holzhey (1989)
Agate	Germany	Lauterbach	3	5.10	8.70	6.73	1.8	*Haake & Holzhey (1989)
Quartz	Germany	Schlottwitz	1	5.9				*Haake *et al.* (1991)
Agate	Germany	Schlottwitz	1	0.3				*Haake *et al.* (1991)
Agate	India	Mardet Bet, Gujarat	15	0.03	0.69	0.23	0.2	Law *et al.* (2012)
Agate	India	Ratanpur, Gujarat	15	0.04	0.65	0.30	0.2	Law *et al.* (2012)
Agate	Iran	Shahr-i-Sokhta	15	0.50	7.43	2.36	1.8	Law *et al.* (2012)
Agate	Mexico	Chihuahua	2	0.3	0.4	0.35	0.1	*Cross (1996)
Quartz	Mexico	Chihuahua	1	0.1				*Cross (1996)
Agate	Namibia	Sarusa Mine	1	0.1				*Harris (1989)
Quartz	Namibia	Sarusa Mine	1	0.1				* Harris (1989)
Jasper	Norway	Ordovician Løkken ophiolite	12	0.05	0.67	0.30	0.2	Grenne & Slack (2005)
Flint	Russia	Moscow, Valdai and White Sea	12	0.22	3.80	1.47	1.5	Olofsson & Rodushkin (2011)
Flint	Sweden	Vuollerim	6	0.02	2.00	0.68	0.8	Olofsson & Rodushkin (2011)
Agate	Thailand	Ban Khao Mogun	20	0.74	42.14	7.29	11.7	Law *et al.* (2012)
Agate	Turkey	Dereyalakvillage, Eskişehir	1	154				Parali *et al.* (2011)
Agate	UK	Ardownie Quarry, Scotland	1	2.8				*Fallick *et al.* (1985)
Quartz	UK	Ardownie Quarry, Scotland	1	3.1				*Fallick *et al.* (1985)
Agate	UK	Montrose, Scotland	1	0.5				*Fallick *et al.* (1985)
Quartz	UK	Montrose, Scotland	1	0.5				*Fallick *et al.* (1985)
Quartzite	USA	Colorado (various sites)	402	–	44.20	1.07	3.5	Pitblado *et al.* (2003)
Total			687	–	260	9.05	30.4	

Abbreviations: N – number of analysed samples; Min. – minimum value; Max. – maximum value; Av. – average value; SD – standard deviation value
*From Götze *et al.* (2001).

https://doi.org/10.1017/S0016756822001200 Published online by Cambridge University Press

6.d.4. Caesium

Cs, Rb and K (LFS elements) show a consistent correlation in several samples. In hydrothermal fluids, the alkali metals such as Rb and Cs remain in solution and are later incorporated into other phases such as micas (see, e.g. Codeço *et al.* 2021). Accordingly, the metamorphic rocks, especially the metapelite A2, turned out to be the most Cs-rich rocks among those examined. The derivation of Cs from water–rock interaction with these rocks thus appears as plausible.

6.e. Gold and iron

As specified above, while the absolute quantities have to be considered with caution, the presence of Au in chalcedonies is evident and not surprising. Au leaching and transport require suitable redox conditions as well as the availability of suitable complexing agents (Mann, 1984; Webster & Mann, 1984; Stoffregen, 1986; Bowell *et al.* 1993; Freyssinet *et al.* 2005). It is commonly believed that, at low temperatures (<400 °C), Au covalently bonds with bisulfide ligand (Wood *et al.* 1987) and is then sequestered by sulfides (Cygan & Candela, 1995; Jugo *et al.* 1999; Simon *et al.* 2000) while, at high temperatures (>350–400 °C), gold tends to form chloride complexes (Candela, 2003). In the first case, the precipitation of gold can occur from the ore-fluids, for example, owing to fluid dilution or fluid–rock interactions, or from the achievement of oxidizing conditions that cause the breakdown of the sulfide complexes (Ilchik & Barton, 1997). In the second case, however, it is cooling that favours the precipitation of gold from gold-chloride solutions (Gammons & Williams-Jones, 1997).

In this regard, it is also worth mentioning the investigation by Williams-Jones & Normand (1997), according to whom Sb and Au jointly reach maximum concentrations when antimony is transported as $HSb_2S_4^-$. The same authors highlight how evident Sb–Au associations are reached when the transport takes place in an alkaline environment (such as limestones) and precipitation occurs in an environment suitable for the acidification of the waters (such as phyllosilicate-rich rocks). In this way, hydrogen ions are produced and can promote the deposition of gold and stibnite. Undoubtedly other processes are possible, but the similarity of the conditions described by Williams-Jones & Normand (1997) to those provided by the area under investigation make this reconstruction one of the most likely.

On the other hand, the absence of correlation of Au with iron seems to diminish (but not exclude) the possible importance of an association with Fe-oxyhydroxide, as often reported in the literature (Karasyova *et al.* 1998; Ran *et al.* 2002; Cohen & Waite, 2004; Corral *et al.* 2018). Moreover, in the territory under examination, the lack of a correlation between stibnite and pyrite occurrences is observed. As explained by Dessau (1952), 'pyrite and stibnite were deposited at the footwall and at the roof of the limestone, respectively, due to the chemical action, together with the drop in temperature and pressure, or due to a chronological shift for which pyrite should have been deposited in a "slightly earlier, higher temperature period"'. In a nutshell, the precipitation of pyrite and Sb–Au should be in succession. While the former lowers the amount of reduced sulfur in the ore fluid, the latter is favoured by a lowering of temperatures able to decrease Sb solubility and lead to Sb–Au precipitation. Finally, it may be interesting to recall the study performed by Nelson (1990), which reports the range of Au concentration in jasperoids (up to 94 ppm) in US Carlin-type orebodies and traces the origin of gold to marine black-shales. Metamorphic rocks and chalcedonies are those bearing discrete Au amounts.

6.f. Textures

The various growth and textures observed in chalcedony testify to the physicochemical variability of the mineralizing solutions, chiefly in terms of SiO_2 concentration and pH (Richter *et al.* 2015). On the other hand, the feathery quartz (jigsaw-puzzle texture) observed in PP8 indicates recrystallization. Dong *et al.* (1995) established that this texture forms at quartz stability temperatures (>180 °C) from the transformation of pre-existing silica phases such as amorphous silica or chalcedony (Lovering, 1972).

The presence of calcite layers in PP4 may indicate a process involving boiling, with consequent loss of CO_2, generation of CO_3^{2-} (from dissociation of HCO_3^-) and precipitation of calcite (Henley & Brown, 1985; Reed & Spycher, 1985). However, the analysis of fluid inclusions performed on other agates from Poggio Peloso by Brogi & Fulignati (2012) did not retrieve evidence of boiling. Otherwise, calcite may have been generated by contact of cold fluids with hot rocks (retrograde solubility; see Simmons & Christenson, 1994).

7. Conclusions

The chalcedonies of Poggio Peloso are the first Sb-rich chalcedonies reported in the literature. Not only is there no comparison among chalcedony and agate analysed to date, but not even the rocks present in the surrounding area have comparably high Sb levels. Antimony is strongly correlated with B, Mn, As and Cs in these chalcedonies. While the high presence of B and Mn may indicate the role of the fluids that, leaching the hosting carbonates, led to their replacement with chalcedony, As and Cs can be better associated with fluids interacting with metamorphic rocks.

The fluid transport in an alkaline environment agrees with the presence of carbonates, whereas silica precipitation in such an environment is possibly confirmed by features such as the abundance of barite inclusions. The latter may be further correlated with and explain the positive Eu anomaly observed in these chalcedonies (as well as in the Palaeozoic metamorphic rocks A1 and A2 from the Monte Amiata geothermal field).

The alkaline environment may also be indicated as responsible for the Sb–Au association, while the acidification of the waters promoted by metamorphic rocks or volatile fluids (HF) and SiF_4, GeF_4 and BF_3 compounds (related to the abundance of Ge) should have favoured their precipitation.

Among the acidic components carried by the fluids, silicic acid must be included. For neither the latter nor any other constituent of these chalcedonies was it possible to draw a convincing correlation with the surrounding volcanic rocks. The comparison established on the basis of the REEs drew significant analogies only with the carbonate (B and Mn seen above) and metamorphic rocks. Among the latter, the Palaeozoic rocks (graphitic quartz-metasandstone and metasiltite and a graphitic phyllite) from two geothermal wells of the Monte Amiata geothermal field provided the most convincing comparison, also regarding the content of gold. In addition, some features of the geothermal fluids of this field (i.e. significant concentration of Sb, B and SiO_2; positive Eu anomaly) seem to be similar to those of the fluid that deposited the chalcedonies. Thus, the latter fluid likely circulated in and reacted with metamorphic rocks analogous to those hosting the deep reservoir of the Monte Amiata geothermal field.

As for the deposition temperatures, it is possible to assume that they did not exceed the threshold of 225 °C, which was set as the

https://doi.org/10.1017/S0016756822001200 Published online by Cambridge University Press

upper term for the deposition of the Poggio Peloso quartz. In any case, the textures of the chalcedonies testify to the physicochemical variability of the mineralizing solutions and different precipitation. Therefore, they are representative of a diachronic process in which fluids with different characteristics have formed different generations of the silica phases.

Supplementary material. To view supplementary material for this article, please visit https://doi.org/10.1017/S0016756822001200

Acknowledgements. The authors would like to thank Enel Green Power S.p.A. for providing the well samples from the Monte Amiata geothermal field and the permission to publish the results. Author contributions: conceptualization, data curation, formal analysis, supervision: EG; investigation: EG, AB; resources: EG, AL; visualization: EG, AB; writing – original draft: EG, AB, GR. All data generated or analysed during this study are included in this published article and its supplementary information files.

Conflict of interest. None.

References

Agosta F, Alessandroni M, Antonellini M, Tondi E and Giorgioni M (2010) From fractures to flow: a field-based quantitative analysis of an outcropping carbonate reservoir. *Tectonophysics* **490**, 197–213. doi: 10.1016/j.tecto.2010.05.005.

Aldinucci M, Brogi A and Sandrelli F (2005) The metamorphic units of the eastern side of Monte Leoni (Northern Apennines, Italy). *Bollettino della Società Geologica Italiana* **124**, 313–32.

Aleksandrova VA, Drits VA and Sokolova GV (1973) Crystal structure of ditrioctahedral chlorite. *Soviet Physics Crystallography* **18**, 50–3.

Bagby WC and Berger BR (1985) Geologic characteristics of sediment-hosted, disseminated precious-metal deposits in the Western United States. In *Geology and Geochemistry of Epithermal Systems* (eds BR Berger and PM Bethke), pp. 169–202. Reviews in Economic Geology vol. 2. Littleton CO: Society of Economic Geologists. doi: 10.5382/Rev.02.08.

Barbier E (2002) Geothermal energy technology and current status: an overview. *Renewable and Sustainable Energy Reviews* **6**, 3–65. doi: 10.1016/S1364-0321(02)00002-3.

Bartole R (1995) The North Tyrrhenian–Northern Apennines post-collisional system: constraints for a geodynamic model. *Terra Nova* **7**, 7–30. doi: 10.1111/j.1365-3121.1995.tb00664.x.

Batini F, Brogi A, Lazzarotto A, Liotta D and Pandeli E (2003) Geological features of Larderello-Travale and Mt. Amiata geothermal areas (southern Tuscany, Italy). *Episodes* **26**, 239–44. doi: 10.18814/epiiugs/2003/v26i3/015.

Bau M (1991) Rare-earth element mobility during hydrothermal and metamorphic fluid-rock interaction and the significance of the oxidation state of europium. *Chemical Geology* **93**, 219–30. doi: 10.1016/0009-2541(91)90115-8.

Beer M (1992) Achate und andere Mineralien aus den nordostböhmischen Melaphyren. *Mineralien Welt* **4**, 47–51.

Berger BR and Silberman ML (1985) Relationships of trace-element patterns to geology in hot-spring-type precious-metal deposits. In *Geology and Geochemistry of Epithermal Systems* (eds BR Berger and PM Bethke), pp. 233–48. Reviews in Economic Geology vol. 2. Littleton CO: Society of Economic Geologists. doi: 10.5382/Rev.02.10.

Bernard-Romero MA, Taran YA and Pennisi M (2010) Geochemistry of boron in fluids of Los Humeros and Los Azufres hydrothermal systems, Mexico. In *Water-Rock Interaction* (eds P Birkle and IS Torres-Alvarado), pp. 145–8. London: Taylor & Francis Group.

Bernoulli D (2001) Mesozoic–Tertiary carbonate platforms, slopes and basins of the external Apennines and Sicily. In *Anatomy of an Orogen: The Apennines and Adjacent Mediterranean Basins* (eds GB Vai and IP Martini), pp. 307–26. Dordrecht: Kluwer Academic Publishers.

Bertini G, Cappetti G and Fiordalisi A (2005) Characteristics of geothermal fields in Italy. *Giornale di Geologia Applicata* **1**, 247–54.

Bingqiu Z, Jinmao Z, Lixin Z and Yaxin Z (1986) Mercury, arsenic, antimony, bismuth and boron as geochemical indicators for geothermal areas. *Journal of Geochemical Exploration* **25**, 379–88. doi: 10.1016/0375-6742(86)90085-3.

Blankenburg H-J (1988) *Achat*. Leipzig: VEB Deutscher Verlag für Grundstoffindustrie.

Boschi C, Dini A, Dallai L, Ruggieri G and Gianelli G (2009) Enhanced CO_2-mineral sequestration by cyclic hydraulic fracturing and Si-rich fluid infiltration into serpentinites at Malentrata (Tuscany, Italy). *Chemical Geology* **265**, 209–26. doi: 10.1016/j.chemgeo.2009.03.016.

Bowell RH, Foster RP and Gize AP (1993) The mobility of gold in tropical rain forest soils. *Economic Geology* **88**, 999–1016. doi: 10.2113/gsecongeo.88.5.999.

Boyle RW and Jonasson IR (1973) The geochemistry of arsenic and its use as an indicator element in geochemical prospecting. *Journal of Geochemical Exploration* **2**, 251–96. doi: 10.1016/0375-6742(73)90003-4.

Braga R (1980) L'antimonite in Toscana: genesi e descrizione dei giacimenti. *Lazio Minerale* **5–7**, 16–26.

Brigatti MF, Frigieri P and Poppi L (1998) Crystal chemistry of Mg-, Fe-bearing muscovites – $2M_1$. *American Mineralogist* **83**, 775. doi: 10.2138/am-1998-7-809.

Brizzi G and Sabelli C (1985) Minerali di Poggio Peloso (GR). *Rivista Mineralogica Italiana* **8**, 135–43.

Brogi A (2006) Foliation relationships and structural facing vs. vergence determinations in refolded low-grade metamorphic rocks: an example from the Tuscan Metamorphic "Basement" (Northern Apennines, Italy). *Journal of Structural Geology* **28**, 115–28. doi: 10.1016/j.jsg.2005.07.009.

Brogi A (2008) Kinematics and geometry of Miocene low-angle detachments and exhumation of the metamorphic units in the hinterland of the Northern Apennines (Italy). *Journal of Structural Geology* **30**, 2–20. doi: 10.1016/j.jsg.2007.09.012.

Brogi A (2011) Bowl-shaped basin related to low-angle detachment during continental extension: the case of the controversial Neogene Siena Basin (central Italy, Northern Apennines). *Tectonophysics* **499**, 54–76. doi: 10.1016/j.tecto.2010.12.005.

Brogi A, Alcicek MC, Liotta D, Capezzuoli E, Zucchi M and Matera PF (2021) Step-over fault zones controlling geothermal fluid-flow and travertine formation (Denizli Basin, Turkey). *Geothermics* **89**, 101941. doi: 10.1016/j.geothermics.2020.101941.

Brogi A and Cerboneschi A (2007) Upper crust "boudinage" during post-collisional Miocene extension in Tuscany: insights from the southern part of the Larderello geothermal area (Northern Apennines, Italy). *Geodinamica Acta* **20**, 327–51. doi: 10.3166/ga.20.327-351.

Brogi A, Fabbrini L and Liotta D (2011) Sb–Hg ore deposit distribution controlled by brittle structures: the case of the Selvena mining district (Monte Amiata, Tuscany, Italy). *Ore Geology Reviews* **41**, 35–48. doi: 10.1016/j.oregeorev.2011.06.004.

Brogi A, Fidolini F and Liotta D (2013) Tectonic and sedimentary evolution of the Upper Valdarno Basin: new insights from the lacustrine S. Barbara Basin. *Italian Journal of Geosciences* **132**, 81–97. doi: 10.3301/IJG.2012.08.

Brogi A and Fulignati P (2012) Tectonic control on hydrothermal circulation and fluid evolution in the Pietratonda–Poggio Peloso (southern Tuscany, Italy) carbonate-hosted Sb-mineralization. *Ore Geology Reviews* **44**, 158–71. doi: 10.1016/j.oregeorev.2011.11.003.

Brogi A and Giorgetti G (2012) Tectono-metamorphic evolution of the siliciclastic units in the Middle Tuscan Range (inner Northern Apennines): Mg–carpholite bearing quartz veins related to syn-metamorphic syn-orogenic foliation. *Tectonophysics* **526–529**, 167–84. doi: 10.1016/j.tecto.2011.09.015.

Brogi A, Lazzarotto A, Liotta D, Ranalli G and Crop-18 Working Group (2005) Crustal structures in the geothermal areas of southern Tuscany (Italy): insights from the CROP 18 deep seismic reflection lines. *Journal of Volcanology and Geothermal Research* **148**, 60–80. doi: 10.1016/j.jvolgeores.2005.03.014.

Brogi A and Liotta D (2008) Highly extended terrains, lateral segmentation of the substratum and basin development: the middle–late Miocene Radicondoli basin (inner northern Apennines, Italy). *Tectonics* **27**, 1–20. doi: 10.1029/2007TC002188.

Brogi A, Liotta D, Capezzuoli E, Matera PF, Kele S, Soligo M, Tuccimei P, Ruggieri G, Yu T-L, Shen C-C and Huntington K (2020) Travertine

deposits constraining transfer zone neotectonic activity in geothermal areas: an example from the inner Northern Apennines (Bagno Vignoni-Val d'Orcia area, Italy). *Geothermics* **85**, 101763. doi: 10.1016/j.geothermics.2019.101763.

Brogi A, Liotta D, Ruggieri G, Capezzuoli E, Meccheri M and Dini A (2016) An overview on the characteristics of geothermal carbonate reservoirs in southern Tuscany. *Italian Journal of Geosciences* **135**, 17–29. doi: 10.3301/IJG.2014.41.

Brookins D (1989) Aqueous geochemistry of rare earth elements. In *Geochemistry and Mineralogy of Rare Earth Elements* (eds BR Lipin and GA McKay), pp. 201–25. Reviews in Mineralogy vol. 21. Berlin: De Gruyter.

Cabioch G, Camoin G, Webb GE, Le Cornec F, Garcia Molina M, Pierre C and Joachimski MM (2006) Contribution of microbialites to the development of coral reefs during the last deglacial period: case study from Vanuatu (South-West Pacific). *Sedimentary Geology* **185**, 297–318. doi: 10.1016/j.sedgeo.2005.12.019.

Cackler PR, Glascock MD, Neff H, Iceland H, Pyburn KA, Hudler D, Hester TR and Chiarulli BM (1999) Chipped stone artefacts, source areas, and provenance studies of the Northern Belize chert-bearing zone. *Journal of Archaeological Science* **26**, 389–97. doi: 10.1006/jasc.1998.0340.

Cady SL, Wenk H-R and Sintubin M (1998) Microfibrous quartz varieties: characterization by quantitative X-ray texture analysis and transmission electron microscopy. *Contributions to Mineralogy and Petrology* **130**, 320–35. doi: 10.1007/s004100050368.

Calcagnile G and Panza G (1981) The main characteristics of the lithosphere asthenosphere system in Italy and surrounding regions. *Pure and Applied Geophysics* **119**, 865–79. doi: 10.1007/BF01131263.

Candela PA (2003) Ores in the Earth's crust. In *Treatise on Geochemistry, Volume 3* (ed. RL Rudnick), pp. 411–31. Oxford: Elsevier. doi: 10.1016/B0-08-043751-6/03028-0.

Capezzuoli E, Ruggieri G, Rimondi V, Brogi A, Liotta D, Alçiçek MC, Alçiçek H, Bülbül A, Gandin A, Meccheri M, Shen C-C and Baykara MO (2018) Calcite veining and feeding conduits in a hydrothermal system: insights from a natural section across the Pleistocene Gölemezli travertine depositional system (western Anatolia, Turkey). *Sedimentary Geology* **364**, 180–203. doi: 10.1016/j.sedgeo.2017.12.012.

Cappetti G, D'Olimpio P, Sabatelli F and Tarquini B (1995) Inhibition of antimony sulphide scale by chemical additives: laboratory and field test results. In *Proceedings of the World Geothermal Congress – Section 11, Corrosion and Scaling, Florence, Italy, 18–31 May 1995*, pp. 2503–7.

Carmignani L, Decandia FA, Disperati L, Fantozzi PL, Kligfield R, Lazzarotto A, Liotta D and Meccheri M (2001) Inner Northern Apennines. In *Anatomy of an Orogen: the Apennines and Adjacent Mediterranean Basins* (eds GB Vai and IP Martini), pp. 197–213. Dordrecht: Kluwer. doi: 10.1007/978-94-015-9829-3_14.

Carmignani L, Decandia FA, Disperati L, Fantozzi PL, Lazzarotto A, Liotta D and Meccheri M (1994) Tertiary extensional tectonics in Tuscany (Northern Apennines, Italy). *Tectonophysics* **238**, 295–315. doi: 10.1016/0040-1951(94)90061-2.

Chao SH, Hargreaves A and Taylor WH (1940) The structure of orthoclase. *Mineralogical Magazine and Journal of the Mineralogical Society* **25**, 498–512. doi: 10.1180/minmag.1940.025.168.05.

Cline JS and Hofstra AA (2000) Ore-fluid evolution at the Getchell Carlin-type gold deposit, Nevada, USA. *European Journal of Mineralogy* **12**, 195–212. doi: 10.1127/ejm/12/1/0195.

Cline JS, Hofstra AH, Muntean JL, Tosdal RM and Hickey KA (2005) Carlin-type gold deposits in Nevada: critical geological characteristics and viable models. In *Economic Geology: One Hundredth Anniversary Volume: 1905–2005* (eds JW Hedenquist, JFH Thompson, R Goldfarb and JP Richards), pp. 451–84. Littleton CO: Society of Economic Geology. doi: 10.5382/AV100.15.

Codeço MS, Weis P, Trumbull RB, Van Hinsberg V, Pinto F, Lecumberri-Sanchez P and Schleicher AM (2021) The imprint of hydrothermal fluids on trace-element contents in white mica and tourmaline from the Panasqueira W–Sn–Cu deposit, Portugal. *Mineralium Deposita* **56**, 481–508. doi: 10.1007/s00126-020-00984-8.

Cohen DR and Waite TD (2004) Interaction of aqueous Au species with goethite, smectite and kaolinite. *Geochemistry: Exploration, Environment, Analysis* **4**, 279–87. doi: 10.1144/1467-7873/04-207.

Cole WF, Sörum H and Kennard O (1949) The crystal structures of orthoclase and sanidinized orthoclase. *Acta Crystallographica* **2**, 280–7. doi: 10.1107/S0365110X49000734.

Corral I, Corbella M, Gómez-Gras D and Griera A (2018) Trace-metal content of the Cerro Quema Au-Cu deposit (Azuero Peninsula, Panama): implications for exploration. *Boletín de la Sociedad Geológica Mexicana* **70**, 549–65.

Craw D, Chappell D and Reay A (2000) Environmental mercury and arsenic sources in fossil hydrothermal systems, Northland, New Zealand. *Environmental Geology* **39**, 875–87. doi: 10.1007/s002549900068.

Cross BL (1996) *The Agates of Northern Mexico*. Edina: Burgess International Group.

Cygan GL and Candela PA (1995) Preliminary study of gold partitioning among pyrrhotite, pyrite, magnetite, and chalcopyrite in gold-saturated chloride solutions at 600 to 700 °C, 140 MPa (1400 bars). In *Magmas, Fluids and Ore Deposits* (ed. JFH Thompson), pp. 129–38. Mineralogical Association of Canada Short Course Series vol. 23. Ottawa: Mineralogical Association of Canada.

Dessau G (1952) Antimony deposits of Tuscany. *Economic Geology* **47**, 397–413.

Dessau G (1977) Die Quecksilber-und Antimonlagerstätten der Toskana. *Freiberger Forschungshefte, Reihe C: Geowissenschaften, Mineralogie-Geochemie* **328**, 47–71.

Dessau G, Duchi G and Stea B (1972) Geologia e depositi minerari della zona Monti Romani-Monteti. *Memorie della Società Geologica Italiana* **11**, 217–60.

Di Stefano R, Bianchi I, Ciaccio MG, Carrara G and Kissling E (2011) Three-dimensional Moho topography in Italy: new constraints from receiver functions and controlled source seismology. *Geochemistry, Geophysics, Geosystems* **12**, Q09006. doi: 10.1029/2011GC003649.

Dill HG, Melcher F and Botz R (2008) Meso- to epithermal W-bearing Sb vein-type deposits in calcareous rocks in western Thailand; with special reference to their metallogenetic position in SE Asia. *Ore Geology Reviews* **34**, 242–62. doi: 10.1016/j.oregeorev.2007.10.004.

Dini A (2003) Ore deposits, industrial minerals and geothermal resources. *Periodico di Mineralogia* **72 (Special Issue)**, 41–52.

Dini A, Gianelli G, Puxeddu M and Ruggieri G (2005) Origin and evolution of Pliocene–Pleistocene granites from the Larderello geothermal field (Tuscan Magmatic Province, Italy). *Lithos* **81**, 1–31. doi: 10.1016/j.lithos.2004.09.002.

Dini A, Westerman DS, Innocenti F and Rocchi S (2008) Magma emplacement in a transfer zone: the Miocene mafic Orano dyke swarm of Elba Island, Tuscany, Italy. In *Structure and Emplacement of High-Level Magmatic Systems* (eds K Thomson and N Petford), pp. 131–48. Geological Society of London, Special Publication no. 302. doi: 10.1144/SP302.10.

Dong G, Morrison G and Jaireth S (1995) Quartz textures in epithermal veins, Queensland; classification, origin and implication. *Economic Geology* **90**, 1841–56. doi: 10.2113/gsecongeo.90.6.1841.

Dumańska-Słowik M, Natkaniec-Nowak L, Kotarba MJ, Sikorska M, Rzymełka JA, Łoboda A and Gaweł A (2008) Mineralogical and geochemical characterization of the "bituminous" agates from Nowy Kościół (Lower Silesia, Poland). *Neues Jahrbuch für Mineralogie, Abhandlungen* **184**, 255–68. doi: 10.1127/0077-7757/2008/0098.

Dumańska-Słowik M, Powolny T, Sikorska-Jaworowska M, Gaweł A, Kogut L and Poloński K (2018) Characteristics and origin of agates from Płóczki Górne (Lower Silesia, Poland): a combined microscopic, micro-Raman, and cathodoluminescence study. *Spectrochimica Acta – Part A: Molecular and Biomolecular Spectroscopy* **192**, 6–15. doi: 10.1016/j.saa.2017.11.005.

Fallick A, Jocelyn J, Donnelly T, Guy M and Behan C (1985) Origin of agates in volcanic rocks from Scotland. *Nature* **313**, 672–4. doi: 10.1038/313672a0.

Fallick AE, Jocelyn J and Hamilton PJ (1987) Oxygen and hydrogen stable isotope systematics in Brazilian agates. In *Geochemistry and Mineral Formation in the Earth Surface: Proceedings of the International Meeting*

on Geochemistry of the Earth Surface and Processes of Mineral Formation, Granada, Spain, 16–22 March 1986 (eds R Rodriguez-Clemente and Y Taedy), pp. 99–117. Madrid: Consejo Superior de Investigaciones Cientificas.

Faulds JE, Coolbaugh MF, Hinz NH, Cashman PH, Kratt C, Dering G, Edwards J, Mayhew B and McLachlan H (2011) Assessment of favorable structural settings of geothermal systems in the Great Basin, western USA. *Geothermal Resources Council Transactions* **35**, 777–84.

Ferguson RB, Traill RJ and Taylor WH (1958) The crystal structures of low-temperature and high-temperature albites. *Acta Crystallographica* **11**, 331–48. doi: 10.1107/S0365110X5800092X.

Filella M, Belzile N and Lett M-C (2007) Antimony in the environment: a review focused on natural waters. III. Microbiota relevant interactions. *Earth-Science Reviews* **80**, 195–217. doi: 10.1016/j.earscirev.2006.09.003.

French MW, Worden RH and Lee DR (2003) Electron backscatter diffraction investigation of length-fast chalcedony in agate: implications for agate genesis and growth mechanisms. *Geofluids* **13**, 32–44. doi: 10.1111/gfl.12006.

Freyssinet PH, Butt CRM and Morris RC (2005) Ore-forming processes related to lateritic weathering. In *Economic Geology: One Hundredth Anniversary Volume: 1905–2005* (eds JW Hedenquist, JFH Thompson, RJ Goldfarb, JP Richards), pp. 681–722. Littleton CO: Society of Economic Geologists. doi: 10.5382/AV100.21.

Gammons CH and Williams-Jones AE (1997) Chemical mobility of gold in the porphyry-epithermal environment. *Economic Geology* **92**, 45–59. doi: 10.2113/gsecongeo.92.1.45.

Gandin A, Giamello M, Guasparri G, Mugnaini S and Sabatini G (2000) The Calcare Cavernoso of the Montagnola Senese (Siena, Italy): mineralogical-petrographic and petrogenetic features. *Mineralogica et Petrographica Acta* **43**, 271–89.

Garland J, Neilson JE, Laubach SE and Whidden KJ (2012) Advances in carbonate exploration and reservoir analysis. In *Advances in Carbonate Exploration and Reservoir Analysis* (eds J Garland, JE Neilson, SE Laubach and KJ Whidden), pp. 1–15. Geological Society of London, Special Publication no. 370. doi: 10.1144/SP370.15.

German CR, Klinkhammer GP, Edmond JM, Mitra A and Elderfield H (1990) Hydrothermal scavenging of rare earth elements in the ocean. *Nature* **345**, 516–8. doi: 10.1038/345516a0.

Gilg HA, Morteani G, Kostitsyn Y, Preinfalk C, Gatter I and Strieder AJ (2003) Genesis of amethyst geodes in basaltic rocks of the Serra Geral Formation (Ametista do Sul, Rio Grande do Sul, Brazil): a fluid inclusion, REE, oxygen, carbon, and Sr isotope study on basalt, quartz, and calcite. *Mineralium Deposita* **38**, 1009–25. doi: 10.1007/s00126-002-0310-7.

Giorgetti G, Goff B, Memmi I and Nieto F (1998) Metamorphic evolution of Verrucano metasediments in Northern Apennines; new petrological constraints. *European Journal of Mineralogy* **10**, 1295–308.

Giraud A, Dupuy C and Dostal J (1986) Behaviour of trace elements during magmatic processes in the crust: application to acidic volcanic rocks of Tuscany (Italy). *Chemical Geology* **57**, 269–88. doi: 10.1016/0009-2541(86)90054-9.

Gliozzo E, Cairncross B and Vennemann T (2019) A geochemical and micro-textural comparison of basalt-hosted chalcedony from the Jurassic Drakensberg and Neoarchean Ventersdorp Supergroup (Vaal River alluvial gravels), South Africa. *International Journal of Earth Sciences* **108**, 1857–77. doi: 10.1007/s00531-019-01737-3.

Götze J, Möckel R, Kempe U, Kapitonov I and Vennemann T (2009) Characteristics and origin of agates in sedimentary rocks from the Dryhead area, Montana, USA. *Mineralogical Magazine* **73**, 673–90. doi: 10.1180/minmag.2009.073.4.673.

Götze J, Möckel R and Pan Y (2020) Mineralogy, geochemistry and genesis of agate—a review. *Minerals* **10**, 1037. doi: 10.3390/min10111037.

Götze J, Möckel R, Vennemann T and Müller A (2016) Origin and geochemistry of agates in Permian volcanic rocks of the Sub-Erzgebirge basin, Saxony (Germany). *Chemical Geology* **428**, 77–91. doi: 10.1016/j.chemgeo.2016.02.023.

Götze J, Nasdala L, Kleeberg R and Wenzel M (1998) Occurrence and distribution of "moganite" in agate/chalcedony: a combined micro-Raman, Rietveld, and cathodoluminescence study. *Contributions to Mineralogy and Petrology* **133**, 96–105. doi: 10.1007/s004100050440.

Götze J, Schrön W, Möckel R and Heide K (2012) The role of fluids in the formation of agates. *Geochemistry* **72**, 283–6. doi: 10.1016/j.chemer.2012.07.002.

Götze J, Tichomirowa M, Fuchs H, Pilot J and Sharp ZD (2001) Geochemistry of agates: a trace element and stable isotope study. *Chemical Geology* **175**, 523–41. doi: 10.1016/S0009-2541(00)00356-9.

Graetsch H (1994) Structural characteristics of opaline and micro-crystalline silica minerals. In *Silica: Physical Behaviour, Geochemistry and Materials Application* (eds PJ Heaney, CT Prewitt and GV Gibbs), pp. 209–32. Reviews in Mineralogy vol. 29. Littleton CO: Mineralogical Society of America. doi: 10.1515/9781501509698-011.

Grenne T and Slack JF (2005) Geochemistry of jasper beds from the Ordovician Løkken ophiolite, Norway—origin of proximal and distal siliceous exhalites. *Economic Geology* **100**, 1511–27. doi: 10.2113/gsecongeo.100.8.1511.

Guggenheim S and Nelson DO (1993) Inferred limitations to the oxidation of Fe in chlorite: a high-temperature single-crystal X-ray study. *American Mineralogist* **78**, 1197–207.

Guichard F, Church TM, Truil H and Jaffrezic H (1979) Rare earths in barites: distribution and effects on aqueous partitioning. *Geochimica et Cosmochimica Acta* **43**, 983–7. doi: 10.1016/0016-7037(79)90088-7.

Haake R, Fischer J and Reissmann R (1991) Über das Achat – Amethyst – Vorkommen von Schlottwitz im Osterzgebirge. *Mineral Welt* **2**, 20–4.

Haake R and Holzhey G (1989) Achate in kugelförmigen Rhyolithen des Rotliegenden im sächsisch-thüringischem Raum. *Chemie der Erde* **49**, 173–83.

Hancock PL, Chalmers RML, Altunel E and Çakir Z (1999) Travitonics: using travertines in active fault studies. *Journal of Structural Geology* **21**, 903–16. doi: 10.1016/S0191-8141(99)00061-9.

Harris C (1989) Oxygen-isotope zonation of agates from Karoo volcanics of the Skeleton Coast, Namibia. *American Mineralogist* **74**, 476–81.

Heaney PJ (1993) A proposed mechanism for the growth of chalcedony. *Contributions to Mineralogy and Petrology* **115**, 66–74. doi: 10.1007/BF00712979.

Heaney PJ and Davis AM (1995) Observation and origin of self-organized textures in agates. *Science* **269**, 1562–5. doi: 10.1126/science.269.5230.1562.

Heaney PJ, Veblen DR and Post JE (1994) Structural disparities between chalcedony and macrocrystalline quartz. *American Mineralogist* **79**, 452–60.

Henley RW (1985) The geothermal framework of epithermal deposits. In *Geology and Geochemistry of Epithermal Systems* (eds BR Berger and PM Bethke), pp. 1–24. Reviews in Economic Geology vol. 2. Littleton CO: Society of Economic Geologists.

Henley RW and Brown KL (1985) A practical guide to the thermodynamics of geothermal fluids and hydrothermal ore deposits. In *Geology and Geochemistry of Epithermal Systems* (eds BR Berger and PM Bethke), pp. 25–44. Reviews in Economic Geology vol. 2. Littleton CO: Society of Economic Geologists.

Ilchik RP and Barton MD (1997) An amagmatic origin for Carlin-type gold deposits. In *Carlin-Type Gold Deposits Field Conference* (eds P Vikre, TB Thompson, K Bettles, O Christensen and R Parratt), pp. 269–88. Society of Economic Geologists Guidebook Series 28.

Johnson MG (1977) *Geology and Mineral Deposits of Pershing County, Nevada*. Reno: Nevada Bureau of Mines and Geology, Bulletin 89, 121 pp.

Jugo PJ, Candela PA and Piccoli PM (1999) Magmatic sulfides and Au:Cu ratios in porphyry deposits: an experimental study of copper and gold partitioning at 850 °C, 100 MPa in a haplogranitic melt – pyrrhotite – intermediate solid solution-gold metal assemblage, at gas saturation. *Lithos* **46**, 573–89. doi: 10.1016/S0024-4937(98)00083-8.

Kamber BS and Webb GE (2001) The geochemistry of late Archaean microbial carbonate: implications for ocean chemistry and continental erosion history. *Geochimica et Cosmochimica Acta* **65**, 2509–25. doi: 10.1016/S0016-7037(01)00613-5.

Karasyova ON, Ivanova LI, Lakshtanov LZ, Lövgren L and Sjöberg S (1998) Complexation of gold(III)-chloride at the surface of hematite. *Aquatic Geochemistry* **4**, 215–31. doi: 10.1023/A:1009622915376.

Kawano M, Shiraki K and Tomita K (1998) Crystal structure of dehydroxylated $2M_1$ sericite and its relationship with mixed-layer mica/smectite. *Clay Science* **10**, 423–41.

Klemm DD and Neumann N (1984) Ore-controlling factors in the Hg-Sb province of southern Tuscany, Italy. In *Syngenesis and Epigenesis in the Formation of Mineral Deposits* (eds A Wauschkuhn, C Kluth and RA Zimmermann), pp. 482–503. Berlin, Heidelberg: Springer-Verlag. doi: 10.1007/978-3-642-70074-3.

Krauskopf KB (1956) Dissolution and precipitation of silica at low temperatures. *Geochimica et Cosmochimica Acta* **10**, 1–26. doi: 10.1016/0016-7037(56)90009-6.

Landmesser M (1984) Das problem der Achatgenese. *Mitteilungen der Pollichia* **72**, 5–137.

Lattanzi P (1999) Epithermal precious metal deposits of Italy–an overview. *Mineralium Deposita* **34**, 630–8. doi: 10.1007/s001260050224.

Law R, Carter A, Bhan K, Malik A and Glascock MD (2012) INAA of agate sources and artifacts from the Indus, Helmand, and Thailand regions. In *South Asian Archaeology 2007: Proceedings of the 19th International Conference of the European Association of South Asian Archaeology, Ravenna, Italy, 2–6 July 2007* (eds D Frenez and M Tosi), pp. 177–84. British Archaeological Reports, International Series no. 2454.

Le Page Y and Donnay G (1976) Refinement of the crystal structure of low-quartz. *Acta Crystallographica Section B: Structural Science, Crystal Engineering and Materials* **32**, 2456–9. doi: 10.1107/S0567740876007966.

Lindsey DA (1977) Epithermal beryllium deposits in water-laid tuff, western Utah. *Economic Geology* **72**, 219–32. doi: 10.2113/gsecongeo.72.2.219.

Liotta D, Brogi A, Ruggieri G and Zucchi M (2021) Fossil vs. active geothermal systems: a field and laboratory method to disclose the relationships between geothermal fluid flow and geological structures at depth. *Energies* **14**, 933. doi: 10.3390/en14040933.

Liotta D, Ruggieri G, Brogi A, Fulignati P, Dini A and Nardini I (2010) Migration of geothermal fluids in extensional terrains: the ore deposits of the Boccheggiano-Montieri area (southern Tuscany, Italy). *International Journal of Earth Sciences* **99**, 623–44. doi: 10.1007/s00531-008-0411-3.

Locardi E and Nicolich R (1982) Geodinamica del Tirreno e dell'Appennino centro-meridionale: la nuova carta della Moho. *Memorie della Società Geologica Italiana* **41**, 121–40.

Lovering TG (1962) The origin of jasperoid in limestone. *Economic Geology* **57**, 861–89. doi: 10.2113/gsecongeo.57.6.861.

Lovering TG (1972) *Jasperoid in the United States; Its Characteristics, Origin, and Economic Significance*. Geological Survey USA Professional Paper, 170. Washington: United States Government Printing Office, 176 pp.

Lovering TG and Heyl AV (1980) *Jasperoids of the Pando area, Eagle County, Colorado*. Geological Survey Bulletin 1474. Washington: United States Government Printing Office, 42 pp.

Mann AW (1984) Mobility of gold and silver in lateritic weathering profiles: some observations from Western Australia. *Economic Geology* **79**, 38–49. doi: 10.2113/gsecongeo.79.1.38.

Marcoux E, Le Berre P and Cocherie A (2004) The Meillers Autunian hydrothermal chalcedony: first evidence of a ~295 Ma auriferous epithermal sinter in the French Massif Central. *Ore Geology Reviews* **25**, 69–87. doi: 10.1016/j.oregeorev.2003.10.001.

Martini I, Ambrosetti E, Brogi A, Aldinucci M, Zwaan F and Sandrelli F (2021) Polyphase extensional basins: interplay between tectonics and sedimentation in the Neogene Siena-Radicofani Basin (Northern Apennines, Italy). *International Journal of Earth Sciences* **110**, 1729–51. doi: 10.1007/s00531-021-02038-4.

Martini IP and Sagri M (1993) Tectono-sedimentary characteristics of late Miocene-Quaternary extensional basins of the northern Apennines, Italy. *Earth-Science Reviews* **34**, 197–233. doi: 10.1016/0012-8252(93)90034-5.

Matera PF, Ventruti G, Zucchi M, Brogi A, Capezzuoli E, Liotta D, Yu TL, Shen CC, Huntington KW, Rinyu L and Kele S (2021) Geothermal fluid variation recorded by banded Ca-carbonate veins in a fault-related, fissure ridge-type travertine depositional system (Iano, southern Tuscany, Italy). *Geofluids* **2021**, 8817487. doi: 10.1155/2021/8817487.

Mazumdar A, Banerjee DM, Schidlowski M and Balaram V (1999) Rare-earth elements and stable isotope geochemistry of early Cambrian chert-phosphorite assemblages from the Lower Tal Formation of the Krol Belt (Lesser Himalaya, India). *Chemical Geology* **156**, 275–97. doi: 10.1016/S0009-2541(98)00187-9.

McCrank GFD, Misiura JD and Brown PA (1981) *Plutonic Rocks in Ontario*. Geological Survey of Canada, Paper 80-23, 171 pp.

McDonough WF and Sun SS (1995) The composition of the Earth. *Chemical Geology* **120**, 223–53. doi: 10.1016/0009-2541(94)00140-4.

McLemore VT (2002) Geology and geochemistry of the Mid-Tertiary alkaline to calcalkaline intrusions in the northern Hueco Mountains and adjacent areas, McGregor Range, southern Otero County, New Mexico. In *Geology of White Sands* (eds V Lueth, KA Giles, SG Lucas, BS Kues, RG Myers and D Ulmer-Scholle), pp. 129–37. New Mexico Geological Society 53rd Annual Fall Field Conference Guidebook 52.

McLemore VT (2010) *Beryllium Resources in New Mexico and Adjacent Areas*. New Mexico Bureau of Geology and Mineral Resources – New Mexico Institute of Mining and Technology, Open-file Report OF-533, 105 pp.

Meccheri M, Moretti A and Volterrani S (1987) The Verrucano structure of Mt. Leoni (Southern Tuscany, Italy): lithostratigraphic preliminary notes and deformative history. Meeting 'Paleozoic stratigraphy, tectonics, metamorphism in Italy', Siena, 13–14 December 1985. *IGCP Project 5, Newsletter* **7**, 71–3.

Merino E, Wang Y and Deloule E (1995) Genesis of agates in flood basalts; twisting of chalcedony fibers and trace-element geochemistry. *American Journal of Science* **295**, 1156–76. doi: 10.2475/ajs.295.9.1156.

Michard A (1989) Rare earth element systematics in hydrothermal fluids. *Geochimica et Cosmochimica Acta* **53**, 745–50. doi: 10.1016/0016-7037(89)90017-3.

Michard A, Albarède G, Michard G, Minster JF and Charlou JL (1983) Rare-earth elements and uranium in high-temperature solutions from East Pacific Rise hydrothermal vent field (138N). *Nature* **303**, 795–7. doi: 10.1038/303795a0.

Minissale A, Magro G, Vaselli O, Verrucchi C and Perticone I (1997) Geochemistry of water and gas discharges from the Mt. Amiata silicic complex and surrounding areas (central Italy). *Journal of Volcanology and Geothermal Research* **79**, 223–51.

Möckel R and Götze J (2007) Achate aus sächsischen Vulkaniten des Erzgebirgischen Beckens. *Veröffentlichungen des Museums für Naturkunde Chemnitz* **30**, 25–60.

Möller P, Dulski P and Morteani G (2003) Partitioning of rare earth elements, yttrium, and some major elements among source rocks, liquid and vapor of Larderello-Travale Geothermal Field, Tuscany (Central Italy). *Geochimica et Cosmochimica Acta* **67**, 171–83. doi: 10.1016/S0016-7037(02)01054-2.

Möller S, Grevemeyer I, Ranero CR, Berndt C, Klaeschen D, Sallares V, Zitellini N and de Franco R (2013) Early-stage rifting of the northern Tyrrhenian Sea Basin: results from a combined wide-angle and multichannel seismic study. *Geochemistry, Geophysics, Geosystems* **14**, 3032–52. doi: 10.1002/ggge.20180.

Möller P, Morteani G, Dulski P and Preinfalk C (2009) Vapour/liquid fractionation of rare earths, Y^{3+}, Na^{+}, K^{+}, NH^{4+}, Cl^{-}, HCO_3^{-}, SO_4^{2-} and borate in fluids from the Piancastagnaio geothermal field, Italy. *Geothermics* **38**, 360–9. doi: 10.1016/j.geothermics.2009.07.003.

Molli G (2008) Northern Apennine–Corsica orogenic system: an updated overview. In *Tectonic Aspects of the Alpine–Dinaride–Carpathian System* (eds S Siegesmund, B Fügenschuh and N Froitzheim), pp. 413–42. Geological Society of London, Special Publication no. 298. doi: 10.1144/SP298.19.

Montini G, Lattanzi P, Ruggieri G, Maineri C and Tanelli G (1995) Il sistema epitermale a Sb–Au di Frassine (Grosseto). *Plinius* **14**, 238–9.

Moreira P and Fernandez R (2015) La Josefina Au–Ag deposit (Patagonia, Argentina): a Jurassic epithermal deposit formed in a hot spring environment. *Ore Geology Reviews* **67**, 297–313. doi: 10.1016/j.oregeorev.2014.12.012.

Moretti A (1991) Stratigrafia e rilevamento geologico dell'area di Monte Leoni —Roselle (Grosseto). *Studi Geologici Camerti* Special Volume **1**, 143–9.

Morteani G, Ruggieri G, Möller P and Preinfalk C (2011) Geothermal mineralized scales in the pipe system of the geothermal Piancastagnaio power plant (Mt. Amiata geothermal area): a key to understand the stibnite, cinnabarite and gold mineralization of Tuscany (central Italy). *Mineralium Deposita* **46**, 197–210. doi: 10.1007/s00126-010-0316-5.

Morteani G, Voropaev A and Grinenko V (2017) Relation of stibnite mineralisation and geothermal fluids in southern Tuscany (central Italy):

an isotope (C, O, H, S) and Rare Earth Element study. *Neues Jahrbuch fur Mineralogie, Abhandlungen* **194**, 279–96. doi: 10.1127/njma/2017/0062.

Moxon T and Reed SJB (2006) Agate and chalcedony from igneous and sedimentary hosts aged from 13 to 3480 Ma: a cathodoluminescence study. *Mineralogical Magazine* **70**, 485–98. doi: 10.1180/0026461067050347.

Müller A, Wanvik JE and Ihlen PM (2012) Chapter 4. Petrological and chemical characterisation of high-purity quartz deposits with examples from Norway. In *Quartz: Deposits, Mineralogy and Analytics* (eds J Götze and R Möckel), pp. 71–118. Berlin, Heidelberg: Springer.

Neder RB, Burghammer M, Grasl T, Schulz H, Bram A and Fiedler S (1999) Refinement of the kaolinite structure from single-crystal synchrotron data. *Clays and Clay Minerals* **47**, 487–94. doi: 10.1346/CCMN.1999.0470411.

Nelson CE (1990) Comparative geochemistry of jasperoids from Carlin-type gold deposits of the western United States. *Journal of Geochemical Exploration* **36**, 171–95. doi: 10.1016/0375-6742(90)90055-F.

Olofsson A and Rodushkin I (2011) Provenancing flint artefacts with ICP–MS using REE signatures and Pb isotopes as discriminants: preliminary results of a case study from northern Sweden. *Archaeometry* **53**, 1142–70. doi: 10.1111/j.1475-4754.2011.00605.x.

Pandeli E, Bertini G and Castellucci P (1991) The tectonic wedges complex of the Larderello area (southern Tuscany, Italy). *Bollettino della Società Geologica Italiana* **110**, 621–9.

Parali L, Garcia Guinea J, Kibar R, Cetin A and Can N (2011) Luminescence behaviour and Raman characterization of dendritic agate in the Dereyalak village (Eskişehir), Turkey. *Journal of Luminescence* **131**, 2317–24. doi: 10.1016/j.jlumin.2011.05.057.

Peccerillo A (2003) Plio-Quaternary magmatism in Italy. *Episodes* **26**, 222–6. doi: 10.18814/epiiugs/2003/v26i3/012.

Peccerillo A, Poli G and Donati C (2001) The Plio-Quaternary magmatism of southern Tuscany and Northern Latium: compositional characteristics, genesis and geodynamic significance. *Ofioliti* **26**, 229–38.

Peng J, Yi H and Xia W (2000) Geochemical criteria of the Upper Sinian cherts of hydrothermal origin on the southeast continental margin of the Yangtze Plate. *Chinese Journal of Geochemistry* **19**, 217–26. doi: 10.1007/BF03166879.

Pinarelli L, Poli G and Santo AP (1989) Geochemical characterization of recent volcanism from the Tuscan magmatic province (Central Italy): the Roccastrada and San Vincenzo centers. *Periodico di Mineralogia* **58**, 67–96.

Pipino G (1988) Manifestazioni aurifere epitermali in Toscana Meridionale. *Bollettino della Associazione Mineraria Subalpina* **25**, 119–26.

Pitblado BL, Cannon MB, Neff H, Dehler CM and Nelson ST (2003) LA-ICP-MS analysis of quartzite from the Upper Gunnison Basin, Colorado. *Journal of Archaeological Science* **40**, 2196–216. doi: 10.1016/j.jas.2012.11.016.

Powolny T, Dumańska-Słowik M, Sikorska-Jaworowska M and Wójcik-Bania M (2019) Agate mineralization in spilitized Permian volcanics from "Borówno" quarry (Lower Silesia, Poland)—microtextural, mineralogical, and geochemical constraints. *Ore Geology Reviews* **114**, 103–30. doi: 10.1016/j.oregeorev.2019.103130.

Radosavljević SA, Stojanović JN, Radosavljević-Mihajlović AS and Vuković NS (2016) (Pb–Sb)-bearing sphalerite from the Čumavići polymetallic ore deposit, Podrinje Metallogenic District, East Bosnia and Herzegovina. *Ore Geology Reviews* **72**, 253–68. doi: 10.1016/j.oregeorev.2015.07.008.

Ran Y, Fu J, Rate AW and Gilkes RJ (2002) Sorption of Au (I, III) complexes on Fe, Mn oxides and humic acid. *Chemical Geology* **185**, 33–49. doi: 10.1016/S0009-2541(01)00393-X.

Reed MH and Spycher NF (1985) Boiling, cooling, and oxidation in epithermal system: a numerical modelling approach. In *Geology and Geochemistry of Epithermal Systems* (eds BR Berger and PM Bethke), pp. 249–72. Reviews in Economic Geology vol. 2. Littleton CO: Society of Economic Geologists.

Richter S, Götze J, Niemeyer H and Möckel R (2015) Mineralogical investigations of agates from Cordón de Lila, Chile. *Andean Geology* **42**, 386–96. doi: 10.5027/andgeoV42n3-a06.

Rimbotti VE (1884) *Descrizione di alcune miniere e punti antimoniferi della Toscana*. Firenze.

Romagnoli P, Arias A, Barelli A, Cei M and Casini M (2010) An updated numerical model of the Larderello–Travale geothermal system, Italy. *Geothermics* **39**, 292–313. doi: 10.1016/j.geothermics.2010.09.010.

Rudnick RL and Gao S (2003) Composition of the continental crust. In *Treatise on Geochemistry, Volume 3* (ed. RL Rudnick), pp. 1–64. Oxford: Elsevier.

Ruggieri G, Giolito C, Gianelli G, Manzella A and Boiron MC (2004) Application of fluid inclusions to the study of Bagnore geothermal field (Tuscany, Italy). *Geothermics* **33**, 675–92. doi: 10.1016/j.geothermics.2003.12.002.

Saunders JA (1990) Oxygen-isotope zonation of agates from Karoo volcanics of the Skeleton Coast, Namibia: discussion. *American Mineralogist* **75**, 1205–6.

Schmitt-Riegraf C (1996) *Magmenentwicklung und spät-bis post-magmatische Alterationsprozesse permischer Vulkanite im Nordwesten der Nahe-Mulde*. Münstersche Forschungen zur Geologie und Paläontologie no. 80. Münster: Verein der Geologie-Studenten in Münster, 251 pp.

Serri G, Innocenti F and Manetti P (1993) Geochemical and petrological evidence of the subduction of delaminated Adriatic continental lithosphere in the genesis of the Neogene–Quaternary magmatism of central Italy. *Tectonophysics* **223**, 117–47. doi: 10.1016/0040-1951(93)90161-C.

Serri G, Innocenti F and Manetti P (2001) Magmatism from Mesozoic to Present: petrogenesis, time-space distribution and geodynamic implications. In *Anatomy of an Orogen: the Apennines and Adjacent Mediterranean Basins* (eds GB Vai and IP Martini), pp. 77–103. Dordrecht: Kluwer.

Shannon RD (1976) Revised effective ionic radii and systematic studies of interatomic distances in halides and chalcogenids. *Acta Crystallographica Section A: Foundations and Advances* **32**, 751–67. doi: 10.1107/S0567739476001551.

Silberman ML and Berger BR (1985) Relationship of trace-element patterns to alteration and morphology in epithermal precious-metal deposits. In *Geology and Geochemistry of Epithermal Systems* (eds BR Berger and PM Bethke), pp. 203–32. Reviews in Economic Geology vol. 2. Littleton CO: Society of Economic Geologists. doi: 10.5382/Rev.02.09.

Sillitoe RH and Brogi A (2021) Geothermal systems in the northern Apennines, Italy: modern analogues of Carlin-style gold deposits. *Economic Geology* **116**, 1491–591. doi: 10.5382/econgeo.4883.

Simmons SF and Christenson BW (1994) Origins of calcite in a boiling geothermal system. *American Journal of Science* **294**, 361–400. doi: 10.2475/ajs.294.3.361.

Simon G, Kesler SE and Essene EJ (2000) Gold in porphyry copper deposits: experimental determination of the distribution of gold in the Cu-Fe-S system at 400° to 700 °C. *Economic Geology* **95**, 259–70. doi: 10.2113/gsecongeo.95.2.259.

Stavrov OD and Khitrov VG (1962) Possible geochemical relationship observed between cesium and boron. *Geochemistry (U.S.S.R.)*, 57–67 (translated from Russian).

Stoffregen R (1986) Observations on the behavior of gold during supergene oxidation at Summitville, Colorado, U.S.A., and implications for electrum stability in the weathering environment. *Applied Geochemistry* **1**, 549–58. doi: 10.1016/0883-2927(86)90062-4.

Tanaka T and Kamioka H (1994) Trace element abundance in agate. *Geochemical Journal* **28**, 359–62. doi: 10.2343/geochemj.28.359.

Tanelli G (1983) Mineralizzazioni metallifere e minerogenesi della Toscana. *Memorie della Società Geologica Italiana* **25**, 91–109.

Tanelli G, Lattanzi P, Ruggieri G and Corsini F (1991) Metallogeny of gold in Tuscany, Italy. In *Brazil Gold '91* (ed. EA Ladeira), pp. 109–14. Rotterdam: Balkema.

Tanelli G and Scarsella A (1990) Tipologia e modellizzazione genetica delle mineralizzazioni aurifere epitermali della Toscana meridionale. *L'industria Mineraria* **11**, 1–9.

Tiepolo M, Bottazzi P, Palenzona M and Vannucci R (2003) A laser probe coupled with ICP – double-focusing sector-field mass spectrometer for in situ analysis of geological samples and U–Pb dating of zircon. *The Canadian Mineralogist* **41**, 259–72. doi: 10.2113/gscanmin.41.2.259.

van Achterbergh E, Ryan CG, Jackson SE and Griffin WL (2001) Data reduction software for LA-ICP-MS: appendix. In *Laser Ablation–ICP–MS in the Earth Sciences: Principles and Applications* (ed. P Sylvester), pp. 239–43. Mineralogical Association of Canada Short Course Series vol. 29. Ottawa: Mineralogical Association of Canada.

Vezzoni S, Dini A and Rocchi S (2016) Reverse telescoping in a distal skarn system (Campiglia Marittima, Italy). *Ore Geology Reviews* **77**, 176–93.

Vitolo S and Cialdella ML (1995) Silica separation from reinjection brines having different composition at Monta Amiata geothermal plant. *In Proceedings*

of the World Geothermal Congress, Florence, Italy, 18–31 May 1996, pp. 2463–66.

Walker JR and Bish DL (1992) Application of Rietveld refinement techniques to a disordered IIb Mg-Chamosite. *Clays and Clay Minerals* **40**, 319–22. doi: 10.1346/CCMN.1992.0400311.

Wang Y and Merino E (1995) Origin of fibrosity and banding in agates from flood basalts. *American Journal of Science* **295**, 49–77. doi: 10.2475/ajs.295.1.49.

Webster JG and Mann AW (1984) The influence of climate, geomorphology and primary geology on the supergene migration of gold and silver. *Journal of Geochemical Exploration* **22**, 21–42. doi: 10.1016/0375-6742(84)90004-9.

Weissberg BG (1969) Gold-silver ore-grade precipitates from New Zealand thermal waters. *Economic Geology* **64**, 95–108. doi: 10.2113/gsecongeo.64.1.95.

White JF and Corwin JF (1961) Synthesis and origin of chalcedony. *American Mineralogist* **46**, 112–9.

Williams-Jones AE and Norman C (1997) Controls of mineral parageneses in the system Fe-Sb-S-O. *Economic Geology* **92**, 308–24. doi: 10.2113/gsecongeo.92.3.308.

Wood SA, Crerar DA and Borscik MP (1987) Solubility of the assemblage pyrite-pyrrhotite-magnetite-sphalerite-galena-gold-stibine-bismuthinite-argentite-molybdenite in H_2O-NaCl-CO_2 solution from 200 to 350°C. *Economic Geology* **82**, 1864–87. doi: 10.2113/gsecongeo.82.7.1864.

Zucchi M (2020) Faults controlling geothermal fluid flow in low permeability rock volumes: an example from the exhumed geothermal system of eastern Elba Island (northern Tyrrhenian Sea, Italy). *Geothermics* **85**, 101765. doi: 10.1016/j.geothermics.2019.101765.

Zucchi M, Brogi A, Liotta D, Rimondi V, Ruggieri G, Montegrossi G, Caggianelli A and Dini A (2017) Permeability and hydraulic conductivity of faulted micaschist in the eastern Elba Island exhumed geothermal system (Tyrrhenian sea, Italy): insights from Cala Stagnone. *Geothermics* **70**, 125–45. doi: 10.1016/j.geothermics.2017.05.007.